

The Control of Apoptotic Death in the Cells of Granulomatous Inflammatory Lesions from Mice with Latent Tuberculous Infection in the *Ex Vivo* Model

Elena Ufimtseva*

Department of Medical Biotechnology, the Research Institute of Biochemistry, 2 Timakova street, Novosibirsk 630117, Russia

Abstract

Tuberculosis is a leading worldwide health problem. The latent, symptom-free stage of tuberculous infection is characterized by the formation of granulomas, specific aggregates of immune cells, predominantly macrophages, containing mycobacteria. The apoptotic death of macrophages containing mycobacteria is considered the main mechanism by which animals and human organisms oppose tuberculous infection and control its development. Previously, we have compared *Mycobacterium*-host cell relationships in individual granuloma cells from mice with latent tuberculous infection and cells from mouse bone marrow and peritoneal cultures infected with BCG vaccine *in vitro* and shown that increased death rates were revealed for macrophages heavily loaded with mycobacteria after acute BCG infection *in vitro*. While in *ex vivo* cultures granuloma macrophages with large numbers of BCG mycobacteria in them were still viable and had neither apoptotic nor necrotic morphology.

Since different specific cellular responses to latent chronic and acute BCG infection in mouse cells were determined, the our aim was to analyze granulomas isolated from the lungs, spleens and bone marrow of Balb/c mice with latent BCG infection for the presence of inducers and markers of apoptotic cell death. In granuloma cells with increased levels of the inducer of apoptosis TNF α , proapoptotic proteins Bax and Bad, death receptor Fas/CD95 and scavenge receptor CD36, we did not observe P53 stabilization or caspase-3 activation in the cytoplasm or nuclei of macrophages and dendritic cells, irrespective of the presence or absence of acid-fast BCG mycobacteria in them. The survival receptor CD30 was detected on the cell membranes of only few granuloma macrophages. However, at later times of tuberculous infection in mice, virtually all macrophages and other granuloma cell types had considerable amounts of the antiapoptotic protein Bcl-2 in the cytoplasm and, probably, mitochondria, in contrast to macrophages from bone marrow cell cultures and peritoneal exudates infected with BCG mycobacteria *in vitro*. Preservation of mitochondrial $\Delta\Psi_m$ during staining of living granuloma macrophages containing large amounts of the Bcl-2 protein was indicative of its involvement in maintaining the integrity of mitochondrial elements and the protection of granuloma cells from death, because in similar experiments the control macrophages that did not have any Bcl-2 protein in them had considerably reduced $\Delta\Psi_m$ and exhibited morphological signs of apoptotic death. Taken together, our results suggest that the antiapoptotic protein Bcl-2 has been proposed to contribute to the viability of granulomas macrophages not only in *ex vivo* culture, but also in the animal organism when faced with mycobacterial, proinflammatory and proapoptotic factors operating in granulomatous inflammatory lesions at various times of latent tuberculous infection in mice.

Keywords: Latent tuberculous infection in mice; Granulomas in *ex vivo* model; BCG mycobacteria; Control of apoptotic cell death

Abbreviations: BCG: *Mycobacterium bovis* bacillus Calmette-Guérin.

Introduction

Macrophages and dendritic cells are host cells for pathogenic mycobacteria, which can invade these cells and persist in them for years or even for decades [1-7]. The latent, symptom-free stage of tuberculous infection is characterized by the formation of granulomas, specific aggregates of immune cells containing mycobacteria [1-3,8-12]. Several potential mechanisms by which mycobacteria can survive in granuloma cells and defy the immune system of the host organism are proposed. First, pathogenic mycobacteria prevent the phagosomes containing them from merging with host cells' lysosomes and cannot thus be destroyed by lysosomal enzymes [9,13-18]. Secondly, in infected cells, mycobacteria can modulate the expression of proinflammatory (TNF α , IFN γ , IL-1) and anti-inflammatory (IL-10) cytokines involved in the formation of cellular responses and a specific immune response of the host organism to infection [5-9,11-12,19-21]. Finally, mycobacteria cause infected cells to die either by apoptosis, which is characterized by loss of cell membrane elements, chromatin condensation, nuclear fragmentation and the formation of apoptotic bodies, or by necrosis, which is characterized

by compromised cell membranes and nuclear envelopes, cytoplasmic swelling and cellular breakdown [22-25]. The apoptotic death of infected macrophages has been proposed to be one of the main mechanisms by which the organism controls tuberculous infection through depopulating pathogenic microorganisms and infected cells [4-5,7-9,25]. By contrast, the necrotic death of infected cells leads to the release of living bacteria into the extracellular environment and further spread of infection throughout animal and human organisms [5,24-28]. At present, autophagy as a way by which host cells eliminate intracellular pathogens during latent chronic tuberculous infection and at its reactivation is extensively studied [5,8,9,23,24,29,30].

*Corresponding author: Elena Ufimtseva, Department of Medical Biotechnology, the Research Institute of Biochemistry, 2 Timakova street, Novosibirsk 630117, Russia, Tel: +79134806211; E-mail: ufim1@ngs.ru

Received November 23, 2016; Accepted December 28, 2016; Published January 05, 2016

Citation: Ufimtseva E (2017) The Control of Apoptotic Death in the Cells of Granulomatous Inflammatory Lesions from Mice with Latent Tuberculous Infection in the *Ex Vivo* Model. Immunome Res 13: 128. doi: [10.4172/17457580.1000128](https://doi.org/10.4172/17457580.1000128)

Copyright: © 2017 Ufimtseva E. This is an open-access article distributed under the terms of the Creative Commons Attribution License, which permits unrestricted use, distribution, and reproduction in any medium, provided the original author and source are credited.

As is known, apoptosis can be induced by external (cytokines, FasL) or internal (compromised DNA and mitochondrial integrity) stimuli that trigger the receptor-mediated and/or mitochondrial pathways of a complex, many-staged process of cell death, which leads to nuclear fragmentation and the formation of apoptotic bodies to be destroyed by macrophages [23-25,31,32]. The extrinsic pathway of apoptosis is mediated by specific death receptors (Fas/CD95, TNFR1/CD120a, to mention a few), which are in the tumor necrosis factor receptor superfamily [23-25,33]. Following ligand-receptor interactions, TNF α protein induces apoptosis through the formation of non-membrane complexes composed of various proteins and procaspase-8, where the latter undergoes auto-proteolysis and generates the active caspase-8 [23-25,31,34,35]. In lymphoid cells, the initiator caspase-8 directly activates procaspase-3, which leads to the death of lymphocytes [31]. In other cell types, caspase-8 basically acts by cleaving Bid protein, the active form of which triggers the homooligomerization of Bax protein on the mitochondrial outer membrane and the formation of pores [36]. At this point, the mitochondrial pathway of apoptosis is activated [36]. As a result, cytochrome *c* translocates, through the pores, from the mitochondrial intermembrane space to the cytoplasm and triggers the formation of a procaspase-9 activating apoptosome. The initiator caspase-9, in turn, activates procaspase-3 [36]. The substrates for the active effector caspase-3 are multiple intracellular proteins, the destruction of which leads to typical morphological and biochemical signs of apoptotic cell death [22-25]. These processes are inhibited by the antiapoptotic proteins Bcl-2 and Bcl-X_L, which act to protect mitochondria from the action of the proapoptotic proteins Bax, Bad, Bak, and Bid [22-25]. Following exposure of cells to genotoxic agents, the P53 protein is stabilized in the cytoplasm [37]. Proapoptotic effects of the P53 protein occur both in the nucleus, by activation of genes for the proapoptotic proteins Fas/CD95 and Bax or suppression of the transcription of the gene for the antiapoptotic protein Bcl-2, and in the cytoplasm, by directly interacting with these proteins in the cells [38-40]. Due to this interaction, cytoplasmic Bax protein undergoes conformational changes, is activated and moves to the mitochondria, on the membrane of which the P53 protein inactivates Bcl-2 protein [38-40]. It was demonstrated [41] that, when nuclear DNA is extensively damaged, a P53-independent pathway of apoptosis can be triggered by induction of expression of the TNF α cytokine and its autocrine interaction with cell death receptors. Bacterial invasion is known to induce TNF α expression in granuloma macrophages, dendritic cells and T lymphocytes [5-12,34,42]. The TNF α cytokine has been proposed to play an important role in the control of tuberculous infection by not only performing proapoptotic functions, but also engaging in leukocyte activation through the CD30 and CD40 receptors on the cell membrane [34,42]. Suppression of the TNF α cytokine or its receptors led to rapid death of mice from tuberculosis following destruction of granuloma organization, the increase of mycobacteria in the organism and immune dysregulation [43-44].

To date, the main results of analysis of relationships between mycobacteria and host cells have been obtained from *in vitro* studies with infecting human and mouse monocyte-derived macrophages or constant cell lines. It has been found that mycobacterial strains have different effects on cell death induction *in vitro* [24]. Non-virulent *Mycobacterium tuberculosis* strain H37Ra and attenuated *Mycobacterium bovis* bacillus Calmette-Guérin (BCG) caused apoptosis of infected macrophages and the elimination of bacteria, while virulent mycobacterial strains (*M. tuberculosis* H37Rv, Erdman and *M. bovis*) actively reproduced in the cells and acted to prevent their death *in vitro* [45-48]. It has also been found that only virulent *M. tuberculosis* H37Rv induced expression of the Mcl-1 protein, an antiapoptotic member of

the Bcl-2 family, after *in vitro* infection of human THP-1 cells [49]. In parallel, a weaker induction of TNF α expression was observed in human and mouse cells following *in vitro* infection with virulent than non-virulent strains [50-52]. Following *in vivo* infection of zebrafish (*Danio rerio*) juveniles with *M. marinum*, mycobacteria spread in their organisms due to the death of some granuloma macrophages and the release of mycobacteria into the extracellular environment, where they were later phagocyted by uninfected macrophages [28,53]. While the formation of granulomas did not depend on TNF α protein at the earliest times of infection, the expression of this cytokine became critical for maintaining the integrity of granuloma structures as infection progressed [28]. Lack of TNF α action on cells due to blockade of TNF α receptors caused increased growth of mycobacteria in granuloma macrophages, necrosis of infected cells and the spread of infection across the fish organisms [27]. Similarly, in the liver of mice treated *in vivo* with antibodies against TNF α protein, a gradual loss of granuloma structure, decreased granuloma size, decreased granuloma macrophage populations, and increased intracellular BCG mycobacteria reproduction were observed [54]. We have previously demonstrated in our model system of monolayer cultures of cells that migrated *ex vivo* from individual granulomas of mice with latent BCG infection [55] that although mouse granuloma macrophages with an increased production of proinflammatory cytokines, growth factors, and CD receptors for cell activation could not eliminate intracellular BCG mycobacteria entirely, they could still control mycobacterial reproduction in host cells both *in vivo* and in *ex vivo* culture, while the mouse bone marrow and peritoneal macrophages that were not activated after BCG infection *in vitro* had increased mycobacterial loads and death rates [55-57]. Nevertheless, the *in vitro*, *ex vivo* and *in vivo* studies performed to date are not enough to completely understand the mechanisms by which mycobacteria persist in cells for long periods of time, particularly, at the latent stage of tuberculous infection.

In the present work, an *ex vivo* model of granulomas from mice with latent tuberculous infection was used to study the expression of inducers, inhibitors and markers of apoptotic cell death relative to mycobacterial loads. In mouse granuloma cells with an increased production of the inducer of apoptosis TNF α , proapoptotic proteins Bax and Bad, death receptor Fas/CD95 and scavenger receptor CD36, neither significant P53 protein stabilization nor caspase-3 activation was observed in the cytoplasm or nuclei of macrophages, irrespective of the presence or absence of BCG mycobacteria in them. The survival receptor CD30 was detected on the cell membranes of only few granuloma macrophages. It was established that most mouse granuloma cells obtained from spleens and lungs at later times of latent tuberculous infection had considerable amounts of the antiapoptotic protein Bcl-2 in the cytoplasm and, probably, mitochondria, irrespective of the presence or absence of BCG mycobacteria in them. In the macrophages from bone marrow cell cultures and peritoneal exudates infected with BCG mycobacteria *in vitro*, no activation of Bcl-2 production was detected throughout 4-120 h of analysis. It was thus proposed that Bcl-2 might be one of the factors that protected cells from death in granulomatous inflammatory lesions not only in *ex vivo* culture, but also in mouse organisms at different times of latent tuberculous infection.

Materials and Methods

Animals

Two-month-old BALB/c male mice were obtained from the Animal Breeding Facility of the Institute of Cytology and Genetics of the Siberian Branch of the Russian Academy of Sciences (Novosibirsk, Russia). Mice were bred and kept under standard vivarium conditions in accordance

with all the known guidelines for laboratory animal care. Animal experiments were conducted in accordance with "The Guidelines for Manipulations with Experimental Animals" issued by the Russian Ministry of Health (guideline 755). All experimental procedures were approved by the Local Ethical Committee of the Research Institute of Biochemistry, Novosibirsk, Russia.

Infection of mice

Mice were infected with a vaccine prepared from an attenuated live strain of *M. bovis* (the Bacillus Calmette-Guérin vaccine, BCG-1, the Institute of Microbiology and Epidemiology, Moscow, Russia) at a dose of 0.5 mg per mouse, which amounted to 3×10^6 viable BCG mycobacteria in 0.9% NaCl solution. Twenty four mice were each infected via tail vein injection with 100 μ l of the suspension and four mice were each infected intraperitoneally with 200 μ l of the suspension.

Isolation and *ex vivo* culture of mouse granulomas

Mice were anesthetized and sacrificed by cervical dislocation. Isolation of granulomas from the spleens, bone marrow and lungs of mice after BCG infection was performed as previously described [55-57]. In brief, bone marrow was flushed from femurs with RPMI 1640 medium with 50 μ g/ml gentamicin (BioloT, St. Petersburg, Russia). The spleens collected from the animals were cut into small pieces in 5 ml of RPMI 1640 medium with 50 μ g/ml gentamicin. For homogenization the dissected lungs were further disrupted by gently pushing the tissue through a metal screen with pores of 1 mm diameter. Granulomas were isolated from the organ homogenates by centrifugation at 150 xg at room temperature. The granuloma pellets in the RPMI 1640 growth medium containing 10% heat-inactivated fetal bovine serum, 2 mM glutamine, and 50 μ g/ml gentamicin (BioloT, St. Petersburg, Russia) were placed at low-medium density to 24-well tissue culture plates (Orange Scientific, Belgium) with glass coverslips at the bottom and cultured in 0.5 ml medium for several days at +37 °C in an atmosphere containing 5% CO₂. Granulomas were isolated from mice 1 and 2 on day 20 following intraperitoneal infection; mice 1 and 2+5 after one month following intraperitoneal and intravenous infection, respectively; mice 1+16 and 21+24 after two months following intravenous infection; and mouse 25 after two months following intraperitoneal infection. The mouse nomenclature used is explained [55-57]. Peritoneal macrophages were isolated from mice after 20 days and mouse 25 after two months following intraperitoneal infection and cultured under the same conditions as the granuloma cells. After isolation of granulomas from the femur bones of mice 1 and 2 after 20 days following BCG infection, the other bone marrow cells from supernatants were cultured under the same conditions as the granuloma cells. The preparations of cultured, as granuloma cells, peritoneal macrophages of normal BALB/c mice without BCG infection were used as the control groups. Isolation of control fibroblasts from fragments of the splenic capsule or lungs from intact BALB/c mice was performed as previously described [55,57].

Cell cultures and infection *in vitro*

Isolation of peritoneal and bone marrow cells from four intact mice and BCG infection of each cell culture were performed as previously described in detail [57]. Three independent experiments on obtaining and studying cells in the control (uninfected) mouse bone marrow and peritoneal cultures and in cell monolayers after 4-120 h of acute BCG infection *in vitro* have been conducted.

Cell staining

At days 2-5 of *ex vivo* culture, granuloma cells on coverslips were

fixed with 4% formaldehyde solution in phosphate buffer saline (PBS, pH 7.4) for 10 min at room temperature. The same procedure was applied to cells in bone marrow cell and peritoneal macrophage cultures at hours 4, 24, 48, 72, 96, and 120 following infection with BCG vaccine *in vitro* and in control cell cultures without infection. The preparations of peritoneal macrophages and spleen and lung fibroblasts from intact BALB/c mice were fixed as granuloma cells and used as the control for the staining of granuloma cells.

The different antibodies and reagents were used for the immunochemical and the immunofluorescence staining: rat monoclonal primary antibodies to mouse TNF α , CD30, and CD11b (BD, USA, 559064, 553824, and eBioscience, USA, 17-0112, respectively) diluted 1:100, 1:25, and 1:250, respectively; mouse monoclonal primary antibodies to mouse Bcl-2, Bad, CD36, and CD95 (BD, USA, 610538, 610391, 552544 and 610197, respectively) diluted 1:200, 1:200, 1:50, and 1:5000, respectively; rabbit polyclonal primary antibodies to mouse Bax and P53 (BD, USA, 554106, and Novocastra, England, NCL-p53-CM5p, respectively) diluted 1:200 and 1:1000, respectively; rabbit monoclonal primary antibodies to mouse active caspase-3 (BD, USA, 559565) diluted 1:200; goat polyclonal FITC-labeled or Alexa 594-conjugated secondary antibodies to rat IgG (Abcam, England, ab6266 and ab150160, respectively) diluted 1:400 and 1:500, respectively; goat polyclonal FITC-labeled or Alexa 555-conjugated secondary antibodies to mouse IgG (Abcam, England, ab7064, and Invitrogen, USA, A21422, respectively) diluted 1:400 and 1:500, respectively; goat polyclonal Alexa 488-conjugated secondary antibodies to rabbit IgG (Abcam, England, ab7064) diluted 1:400; goat polyclonal biotin-conjugated secondary antibodies to mouse, rabbit, and rat IgG (Sigma, USA, B7264, B7389, and BD, USA, 559286, respectively) diluted 1:100, 1:100, and 1:50, respectively; horseradish peroxidase-conjugated streptavidin (Sigma, USA, S5512), diaminobenzidine (Sigma, USA, D3939), MitoTracker Deep Red FM (Invitrogen, USA, M22426), acidotropic dye LysoTracker Red DND-99 (Invitrogen, USA, L7528).

In the experiments using MitoTracker Deep Red FM, the cell preparations were incubated with 500 nM of the dye for 30 min at +37°C in 5% CO₂ before fixation. The cell preparations were fixed as described above, washed with PBS, permeabilized within 2 min in 0.3% Triton-X100 solution, blocked in PBS solution containing 2% BSA, and finally incubated first with mouse monoclonal primary antibodies to mouse Bcl-2, then with FITC-conjugated goat anti-mouse Ig secondary antibodies.

In the experiments using LysoTracker Red DND-99, the cell preparations were incubated with 50 nM of the acidotropic dye for 5 min at +37°C in 5% CO₂ before fixation. The cell preparations were fixed as described above, washed with PBS, blocked in PBS solution containing 2% BSA, and finally incubated first with mouse monoclonal primary antibodies to CD36, then with FITC-conjugated goat anti-mouse Ig secondary antibodies.

Some of the fixed cell preparations were washed with PBS, treated within 2 min in 0.3% Triton-X100 solution, blocked in PBS solution containing 2% BSA, and finally incubated first with primary specific antibodies to mouse TNF α , Bax, Bad, P53, active caspase-3, and Bcl-2. Specific immunochemical staining of some cell preparations was visualized using secondary goat polyclonal biotin-conjugated antibodies to mouse, rabbit, and rat IgG, then with horseradish peroxidase-conjugated streptavidin and diaminobenzidine solution containing 0.05% H₂O₂. The cells were further counterstained with 1% methyl green. Fluorescent visualization of TNF α and Bcl-2 was enabled using secondary goat polyclonal Alexa 594-conjugated antibodies to rat IgG and FITC-labeled antibodies to mouse IgG, respectively.

Some of the fixed cell preparations were washed with PBS, blocked in PBS solution containing 2% BSA, and incubated first with primary specific antibodies to mouse CD30, CD36, and CD95, and then with secondary goat polyclonal biotin-conjugated antibodies to mouse and rat IgG, then with horseradish peroxidase-conjugated streptavidin and diaminobenzidine solution containing 0.05% H₂O₂. The cells were further counterstained with 1% methyl green. Fluorescent visualization of CD95 was enabled using goat polyclonal Alexa 555-conjugated secondary antibodies to mouse IgG.

Some of the fixed cell preparations were washed with PBS, blocked in PBS solution containing 2% BSA, and incubated with rat monoclonal APC-conjugated primary antibodies to mouse CD11b. After staining for CD, the cell preparations were washed with PBS, treated within 2 min in 0.3% Triton-X100 solution, and incubated with rabbit polyclonal primary antibodies to mouse P53, and then with secondary goat polyclonal Alexa 488-conjugated antibodies to rabbit IgG.

Some of the fixed cell preparations were washed with PBS, blocked in PBS solution containing 2% BSA, and incubated first with rat monoclonal primary antibodies to mouse CD30 and mouse monoclonal primary antibodies to mouse CD95, then with secondary goat polyclonal Alexa 594-conjugated antibodies to rat IgG and FITC-labeled antibodies to mouse IgG.

Some of the fixed cell preparations were washed with PBS, blocked in PBS solution containing 2% BSA, and incubated with mouse monoclonal primary antibodies to mouse CD36. After staining for CD, the cell preparations were washed with PBS, treated within 2 min in 0.3% Triton-X100 solution, and incubated with rat monoclonal primary antibodies to mouse TNF α , and then with secondary goat polyclonal Alexa 594-conjugated antibodies to rat IgG and FITC-labeled antibodies to mouse IgG.

Some of the fixed cell preparations were washed with PBS, treated within 2 min in 0.3% Triton-X100 solution, blocked in PBS solution containing 2% BSA, and incubated with rabbit polyclonal primary antibodies to mouse Bax and mouse monoclonal primary antibodies to mouse Bad. Fluorescent visualization of Bax and Bad was enabled using secondary goat polyclonal Alexa 488-conjugated antibodies to rabbit IgG and Alexa 555-conjugated antibodies to mouse IgG, respectively.

Some of the fixed cell preparations were washed with PBS, treated within 2 min in 0.3% Triton-X100 solution, blocked in PBS solution containing 2% BSA, and incubated first with mouse monoclonal primary antibodies to mouse Bcl-2 and rat monoclonal primary antibodies to mouse TNF α , then with secondary goat polyclonal Alexa 555-conjugated antibodies to mouse IgG and FITC-labeled antibodies to rat IgG.

Some of the fixed cell preparations were washed with PBS, treated within 2 min in 0.3% Triton-X100 solution, blocked in PBS solution containing 2% BSA, and incubated with mouse monoclonal primary antibodies to mouse Bcl-2 and rabbit specific antibodies to mouse Bax, P53, or active caspase-3, then with secondary goat polyclonal Alexa 555-conjugated antibodies to mouse IgG and Alexa 488-conjugated antibodies to rabbit IgG.

The cell preparations were incubated with the appropriate antibodies for 60 min at room temperature. Fluorescent staining was analyzed using the VECTASHIELD[®] Mounting Medium with DAPI (4',6-diamidino-2-phenylindole) (Vector Laboratories, USA, H-1200).

The confocal images of the cells were recorded; the preparations were washed from VECTASHIELD[®] Mounting Medium in PBS for

20 min and re-stained for acid-fast mycobacteria using the Ziehl-Neelsen stain. The cells stained by Ziehl-Neelsen method were further counterstained with 1% methylene blue.

Staining of live cells

After 72 h of *ex vivo* culture, coverslips with granuloma cells from infected mouse 23 or with control peritoneal macrophages were transferred from culture plates to Petri dishes and washed with PBS. Fc receptors on the cells were blocked by incubating the preparations in non-diluted bovine serum (BioloT, St. Petersburg, Russia) for 10 min at +37°C in 5% CO₂. Next, the cell preparations were incubated with mouse monoclonal primary antibodies to mouse Bcl-2 (BD, USA, 610538) diluted 1:50, and, after washing with PBS, with Alexa 555-conjugated goat anti-mouse IgG secondary antibodies (Invitrogen, USA, A1422) diluted 1:400. The cell preparations were incubated with the appropriate antibodies diluted in PBS solution containing 15% fetal bovine serum for 30 min at +37°C in 5% CO₂. Next, after washing with PBS, the cell preparations were incubated with 50 nM DiOC₆ (3,3'-dihexyloxycarbocyanine iodide, Sigma, USA, D273) in PBS solution for 20 min at +37°C in 5% CO₂. Finally, the cell preparations washed with PBS were fixed with 8% formaldehyde solution in PBS for 5 min at room temperature and immediately analyzed using the VECTASHIELD Mounting Medium with DAPI under a laser scanning confocal microscope.

Microscopy

The cytological preparations were examined at the Shared Center for Microscopic Analysis of Biological Objects of the Institute of Cytology and Genetics, SB RAS, using an Axioscop 2 *plus* microscope (Zeiss) and objectives with various magnifications (Zeiss), and photographed using an AxioCam HRc camera (Zeiss); the images were analyzed using the AxioVision 4.7 microscopy software (Zeiss). Cell preparations were stained with fluorescent dyes and examined under an LSM 510 or an LSM 780 laser scanning confocal microscope (Zeiss) using the LSM Image Browser and ZEN 2010 software (Zeiss). Granuloma cells were counted separately on each coverslip for each mouse in each test. In each experiment with bone marrow and peritoneal cell cultures, more than 1000 cells were analyzed at each time point. More than 1000 cells were analyzed at each experiment with control peritoneal macrophages and fibroblasts.

Statistical analysis

Statistical data processing was performed using MS Excel 2007 (Microsoft). Differences were tested for significance using Student's *t*-test.

Results

The inducer of apoptosis TNF α in granuloma cells from mice with latent tuberculous infection and in bone marrow macrophages after BCG infection *in vitro*

The production of the proinflammatory cytokine TNF α was analyzed in the cells of granulomas from spleens isolated after day 20 (/20 d; this is how long it takes mice to develop adaptive immunity to BCG [54]), one month (1 m) and two months (2 m) following infection denoted as Gran/20 d, Gran/1 m, and Gran/2 m, respectively. Because none of the mice was observed to have any sign of acute tuberculous infection at the time of granuloma isolation, it was concluded that these granulomas were isolated at the latent stage of BCG infection. Monolayer cultures of cells that had migrated from each granuloma were obtained. Any of the

monolayer cultures of granuloma cells that may or may not retain cell clusters in the center of granulomatous lesions will be referred to as the “granuloma” throughout. The cellular composition of each granuloma and the mycobacterial loads in granuloma cells from different mice, the expression of various surface markers, and the production of various proinflammatory cytokines and growth factors by mouse granuloma cells were characterized previously [55-57].

Analysis of the production of the proinflammatory cytokine and inducer of apoptosis TNF α using specific antibodies revealed a large number of macrophages and dendritic cells containing this marker in the granulomas of mice at various times of latent tuberculous infection (Figures 1A-1C and 2). The largest number of TNF α -producing macrophages (>70% of the population size) was in the granuloma cells from mice after 20 days following infection with the BCG vaccine *in vivo* (Figure 2). The cells of granulomas from mice after one month and two months following BCG infection *in vivo* showed an about twofold decrease in TNF α -containing cells (Figure 2). A small number of control peritoneal macrophages had TNF α protein (Figure 2) and stained for this marker much less stronger than granuloma cells (Figure 1B). In granuloma macrophages, TNF α protein appeared as dots scattered around perinuclear areas and throughout the cytoplasm, irrespective of the presence or absence of BCG mycobacteria (Figures 1A-1C). Cells inside compacted granuloma structures expressed TNF α protein, too (Figure 1B). All granuloma neutrophils had cytoplasmic TNF α protein. In megakaryocytes, TNF α protein was observed in small cytoplasmic areas. Like control lung and spleen fibroblasts, granuloma platelets and fibroblasts did not stain for TNF α protein either (Figures 1A-1C). No TNF α expression was detectable in mouse 25 peritoneal macrophages isolated after two months following intraperitoneal infection with BCG (Figure 2). The number of TNF α -positive cells did not appear different between the peritoneal macrophages isolated from mice after 20 days following intraperitoneal infection with BCG *in vivo* and from control cultures (Figure 2).

Mouse bone marrow cell cultures that were infected with BCG *in vitro* and had increased mycobacterial loads and death rates in bone marrow macrophages [57] showed a gradual increase in TNF α -producing macrophages (from $3.88 \pm 1.36\%$ at hour 4 and $8.32 \pm 1.86\%$ at hour 24 h of analysis to $12.12 \pm 1.27\%$ at hour 48) (Figure 1D). The number of TNF α -positive macrophages in the control bone marrow cells was unchanged during culture (on average, $4.2 \pm 1.47\%$ throughout hours 4-48 of analysis).

All spleen granulomas from all experimental mice studied were found to contain a considerable number of infected and uninfected macrophages that had no morphological signs of apoptosis or necrosis, their cytoplasm staining for TNF α protein, often very intensely.

Expression of the activation receptor CD30, scavenge receptor CD36 and death receptor Fas/CD95 in mouse granuloma cells

The effect of the TNF α protein on cell viability is known to depend on a variety of factors. An important role in setting up the program for TNF α protein is given to cell receptors, including CD30, a member of the survival receptor subgroup of the TNF α receptor superfamily [42]. Staining with specific antibodies revealed CD30 on the membrane of about one-third of macrophages in mouse spleen granulomas isolated at different times of latent infection, but not in the control peritoneal macrophages (Figure 2, Figures 3A and 3B). CD30-positive cells were detected both among macrophages that had migrated from granulomas and among those that resided in compacted granuloma structures (Figure 3A). We note that the intensity of macrophage staining for

CD30 varied considerably in the same granulomas and did not depend on the presence or absence of BCG mycobacteria in them: while some cells had bright microdomain staining across the cell membranes, some had a small number of dot-sized domains (Figures 3A and 3B). Some dendritic cells in the granulomas had CD30, too; however, their population was half the size of that of CD30-positive granuloma macrophages (Figure 2). Like control fibroblasts, granuloma fibroblasts did not stain for CD30, nor was this antigen detected in granuloma megakaryocytes or platelets (Figure 3A). The CD30 receptor is known to be an important activation marker of T and B lymphocytes, and its transient expression in these cells is associated with antiapoptotic effects and suppression of functions of cytotoxic T lymphocytes [58]. No lymphocytes with the CD30 marker on their surfaces were observed in peritoneal macrophage cultures (both control and those obtained on day 20 following BCG infection *in vivo*) or in mouse granulomas at any time of latent tuberculous infection (Figures 3A and 3B). Therefore, CD30 activation appears to be more important for macrophages and dendritic cells in mouse granulomas, also probably for regulation of TNF α action in them.

In our previous studies [55-57], we observed mouse granuloma macrophages to actively digest and destroy lymphocytes that had morphological signs of apoptotic death. As is known, phagocytosis of cells dead by apoptosis involves the multifunctional scavenger receptor CD36 jointly with the $\alpha\beta3$ integrin receptor and thrombospondins. It has also been proposed [59] that thrombospondin 1 binding to CD36 can induce protein kinase signaling cascades on the cell membrane, which leads to caspase activation-mediated apoptotic death of these cells. The use of specific antibodies that detect CD36 revealed this marker on the membranes of a large number of macrophages, dendritic cells and lymphocytes in granulomas isolated from the spleens of mice after two months following infection with BCG vaccine *in vivo* (Figures 2 and 3C). In control peritoneal macrophages, the membrane of only a small number of cells stained for CD36, less strongly at that (Figures 2 and 3C). Curiously, the number of CD36-positive macrophages did not appear to be different between Gran/1 m and control peritoneal macrophages (Figure 2). The number of CD36-positive cells did not appear to be different between peritoneal macrophages isolated from mice on day 20 following intraperitoneal infection with BCG and control peritoneal macrophages and did not depend on the presence of BCG mycobacteria in the cells (Figures 2 and 3D). Like control lung and spleen fibroblasts, granuloma fibroblasts did not have the CD36 receptor (Figure 3C). All granuloma platelets stained for CD36 intensely; however, this receptor was observed to be virtually absent from granuloma megakaryocytes (Figure 3C). As is known, the glycoprotein CD36 is a receptor for the thrombospondin 1 protein, which is involved in the signaling pathways and interactions of megakaryocytes and platelets, and, therefore, is one of the markers of later stages of their differentiation [60]. Overall, the mouse granuloma macrophages with increased CD36 numbers had a propensity not only to digest dead lymphocytes and platelets in the granulomas, but also to be destroyed via caspase-dependent mechanisms of apoptosis during latent tuberculous infection.

The death receptor Fas/CD95, which induces apoptosis when binding to the Fas/CD95 ligand, was found on the membranes of a large number of granuloma cells from the spleens of all the mice assayed (Figure 2, and Figures 3E and 3F). Most macrophages (whether infected or not), dendritic cells, lymphocytes and neutrophils in granulomas showed a bright microdomain staining for Fas/CD95, often across cell membranes (Figures 3E and 3F). Some granuloma fibroblasts and megakaryocytes had this receptor, too (Figures 3E and

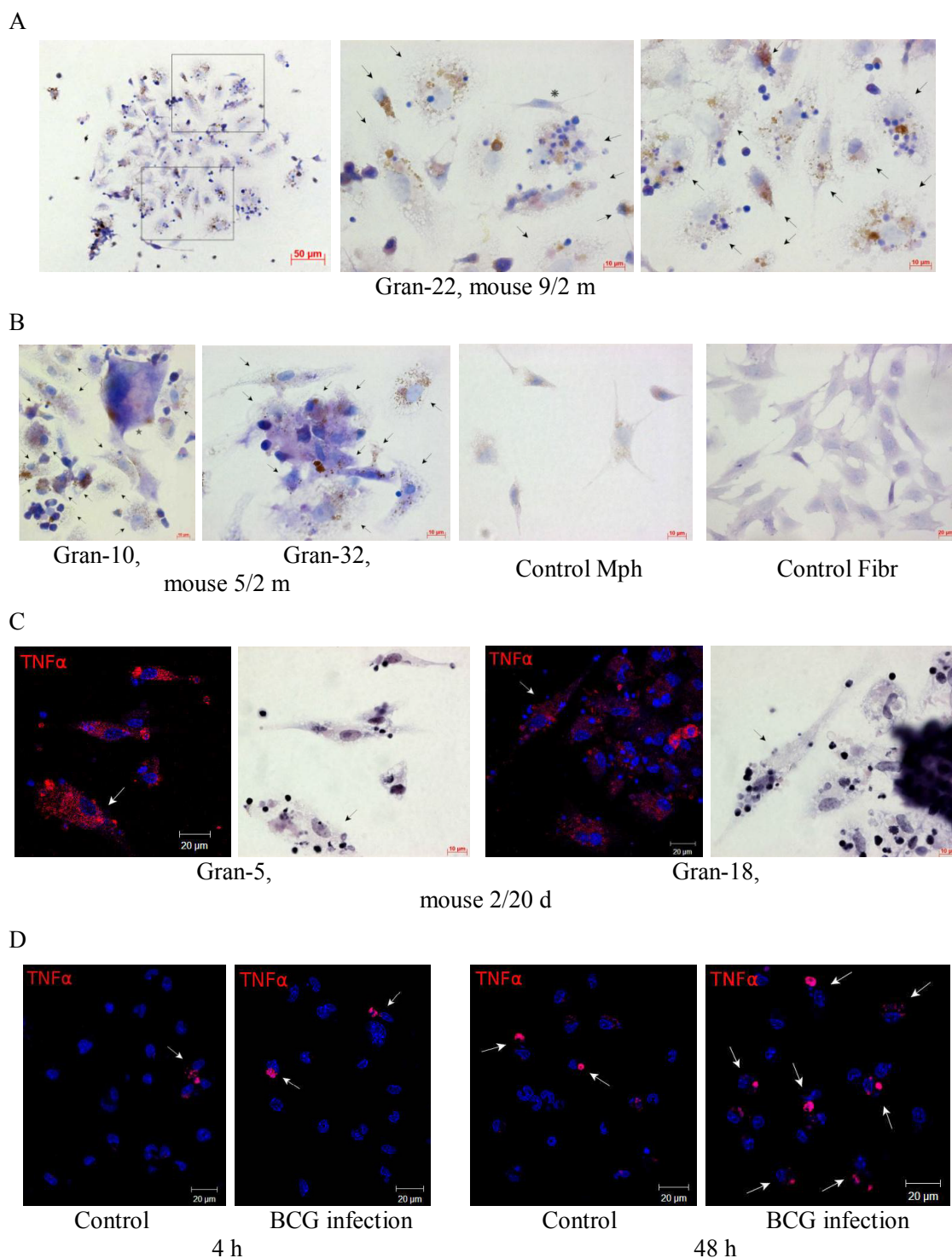


Figure 1: The cells with TNFα protein in (A-C) the fragments of mouse granulomas (Gran) obtained from the spleens of mice after 20 days (20 d) and two months (2 m) following infection with the BCG vaccine *in vivo* and after *ex vivo* culture for several hours, and in (D) the bone marrow macrophages following infection with the BCG vaccine *in vitro* and after culture for several hours. The scale bars are (A, left panel) 50 μm, ((B, right panel) and ((C, left and central right panels), D) 20 μm each, and (other panels) 10 μm each. (A-B) Immunohistochemical localization of TNFα in granuloma cells and control mouse peritoneal macrophages (Mph) and splenic fibroblasts (Fibr). The brown color indicates the presence of TNFα in these cells. An TNFα-producing macrophages and megakaryocyte are indicated by the black arrows and star, respectively; black snowflake indicates fibroblast, that do not contain the antigen. The pictures of granuloma fragments (A, right-central and right panels) are enlarged images of the areas defined by black boxes in picture (A, left panel). (C-D) Confocal immunofluorescent localization of TNFα (red signal) in the cells. Nuclei stained by DAPI (blue signal). (C) In the left central and right panels: the same fragments as in the other panels re-stained for acid-fast BCG mycobacteria by the Ziehl-Neelsen (ZN) method. A TNFα-producing macrophages with BCG mycobacteria are indicated by the white arrows on the fluorescent images and the black arrows on the ZN images. (D) A TNFα-producing bone marrow cells are indicated by the white arrows.

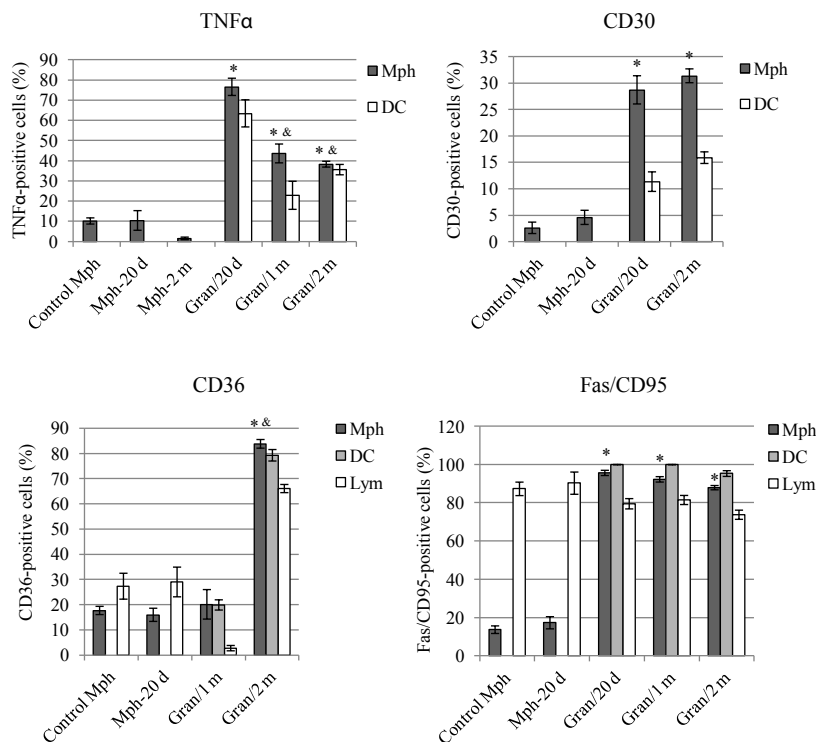


Figure 2: Macrophages (Mph), dendritic cells (DC), and lymphocytes (Lym) with TNF α , CD30, CD36, and Fas/CD95. The objects examined are control peritoneal macrophages from three intact mice, peritoneal macrophages obtained from two mice on 20 day following intraperitoneal infection with the BCG vaccine (Mph-20 d), peritoneal macrophages obtained from mouse 25 after two months following intraperitoneal infection with the BCG vaccine (Mph-2 m), and granulomas from the spleens of two to four mice after 20 days (Gran/20 d), one month (Gran/1 m) and two months (Gran/2 m) following BCG infection *in vivo* and *ex vivo* culture for several hours. Granuloma cells producing various antigens were analyzed in each granuloma separately; the values were averaged all the mice and then combined for granulomas in each group. Data are expressed as the means \pm SEM. * $P < 0.01$ (comparisons of the number of TNF α - or CD-positive macrophages in each Gran group and controls, Mph-20 d, Mph-2 m).

3F). Especially high amounts of Fas/CD95 were observed in granuloma platelets and erythrocytes (Figures 3E and 3F). Cells aggregated inside dense granuloma structures stained for Fas/CD95 as brightly as cells that had migrated from granulomas (Figure 3E and 3F). In the control peritoneal macrophages, Fas/CD95 was detected on the membrane of only a small number of cells, while most lymphocytes had this marker (Figure 2, Figures 3E and 3F). Control lung and spleen fibroblast cultures did not stain for Fas/CD95. We note that the number of Fas/CD95-positive macrophages in bone marrow cell cultures infected *in vitro* did not change throughout 4-48 h of analysis and was $4.77 \pm 1.25\%$ on average, which was as many as there was in the control bone marrow cell cultures (data not shown). Thus, most mouse granuloma cells had increased Fas/CD95 and, therefore, were prepared for induction of apoptosis by one of receptor-mediated mechanisms.

The Bax, Bad and P53 proteins, markers of apoptotic cell death, in mouse granuloma cells

To observe relevant proteins, we used antibodies that detect their regular forms, not conformationally changed or phosphorylated. We found the presence of Bax and Bad proteins in large amounts in all the cells of all granulomas studied from the spleens of mice after one month (3 mice) and two months (9 mice) following infection with the BCG vaccine *in vivo* (Figures 4A-4D). All control peritoneal macrophages, as well as all control lung and spleen fibroblasts, had these antigens; however, they stained much less strongly than granuloma cells (Figures 4A-4D). Staining for Bax protein was observed both across

the cytoplasm of granuloma macrophages and dendritic cells and in small roundish entities of varying size scattered peripherally to the nucleus, where Bax protein showed colocalization with Bad protein (Figure 4D). As is known, Bax and Bad are constitutive proteins in mammalian cells and are present in the cytoplasm at all times [31]. When the cell is exposed to an apoptosis stimulus, Bax protein undergoes conformational changes, moves from the cytoplasm to the mitochondrial outer membrane, interacts with dephosphorylated Bad protein and thus abrogates the antiapoptotic functions of the Bcl-2 and/or Bcl-X_L proteins on the mitochondrial membranes [31]. It has been proposed [36,61] that the balance between Bax, Bad, Bcl-2 and/or Bcl-X_L proteins in the complex on the mitochondrial outer membrane is critical for what follows. Will cell death be prevented? Or will the apoptotic program (mitochondrial membrane permeabilization, the release of apoptogenic factors from the intermembrane space and, eventually, activation of the executioner caspase-3) continue? Thus, the colocalization of the Bax and Bad proteins is indicative of their joint proapoptotic activity in the granuloma cells of mice with latent tuberculous infection.

As is known [38-40], the P53 protein is continuously synthesized in mammalian cells, but is a short-lived protein and degrades rapidly within the complex with the Mdm2 protein, which functions as the ubiquitin ligase. In the cells damaged by genotoxic agents, this complex dissociates, P53 protein is stabilized and escapes proteasome-dependent degradation. As a result, P53 protein can accumulate in the cytoplasm and nuclei and launch the program of a stress-dependent

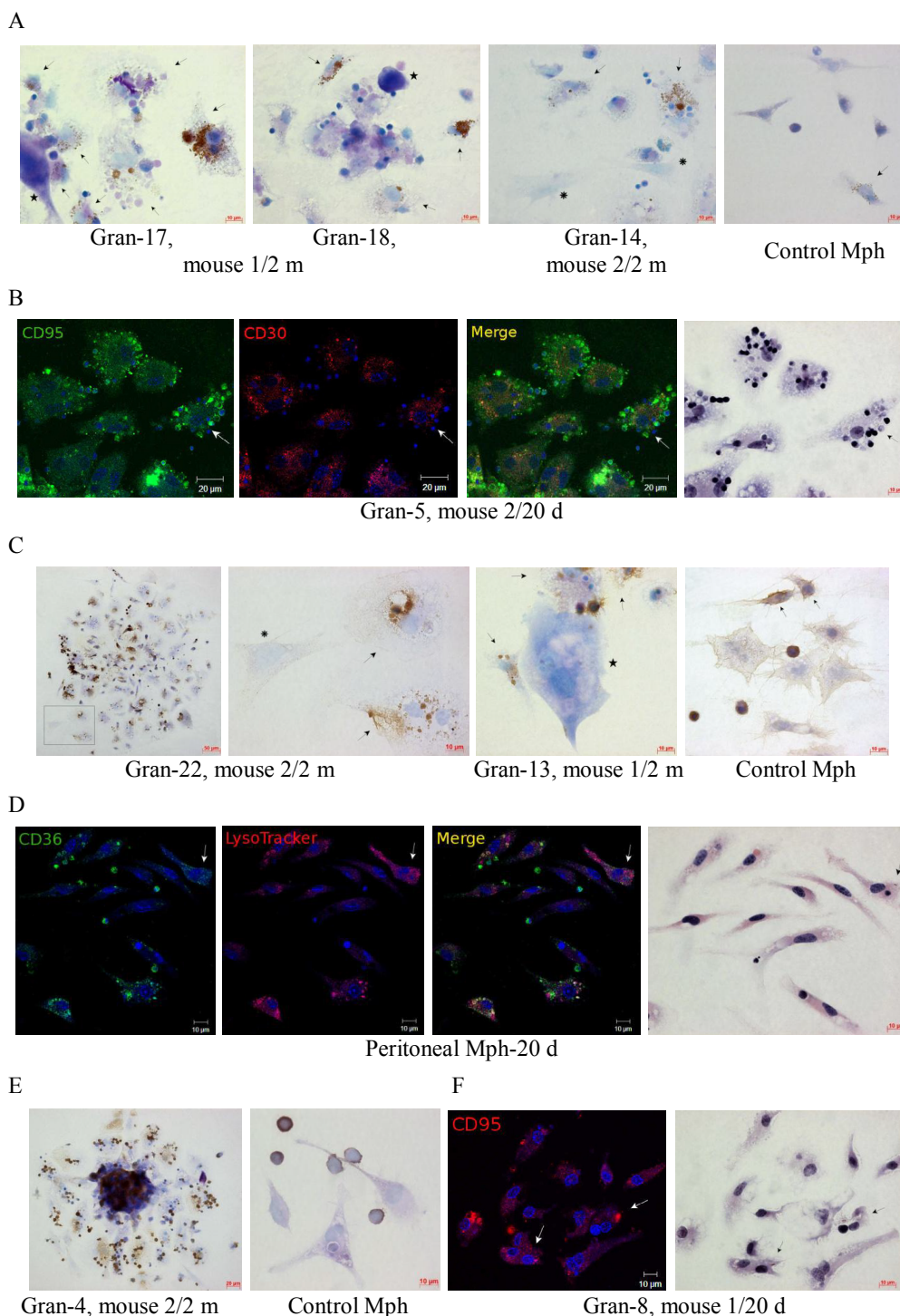


Figure 3: The cells with cell-surface markers (A-B) CD30, (C-D) CD36, and (B, E-F) Fas/CD95 in (A-C, E-F) the fragments of mouse splenic granulomas (Gran) and control mouse peritoneal macrophages (Mph), and (D) peritoneal macrophages obtained from mouse on 20 day following intraperitoneal infection with the BCG vaccine. The scale bars are (C, left panel) 50 μ m, ((B, left, left and right central panels) and (F, left panel)) 20 μ m each, and (other panels) 10 μ m each. (A, C, E) The brown color indicates the presence of various surface antigens on the cells after immunochemical staining. CD-producing macrophages are indicated by the black arrows; black snowflakes and stars indicate fibroblasts and megakaryocytes, respectively, that do not contain the antigen. (B, D, F) Confocal immunofluorescent localization of CD-markers in the cells. Colocalization of the markers on the confocal images of cells (yellow signal). Nuclei stained by DAPI (blue signal). In the right panels: the same fragments as in the other panels re-stained for acid-fast BCG mycobacteria by the ZN method. (B) The granuloma macrophage with BCG mycobacterium, CD95 (green signal) and CD30 (red signal) is indicated by the white arrows on the fluorescent images and the black arrow on the ZN image. (D) The peritoneal macrophage with BCG mycobacterium, CD36 (green signal) and LysoTracker Red DND-99 dye (red signal) is indicated by the white arrows on the fluorescent images and the black arrow on the ZN image. (F) The granuloma macrophages with BCG mycobacteria reproducing in it and CD95 (red signal) are indicated by the white arrows on the fluorescent image and the black arrows on the ZN image.

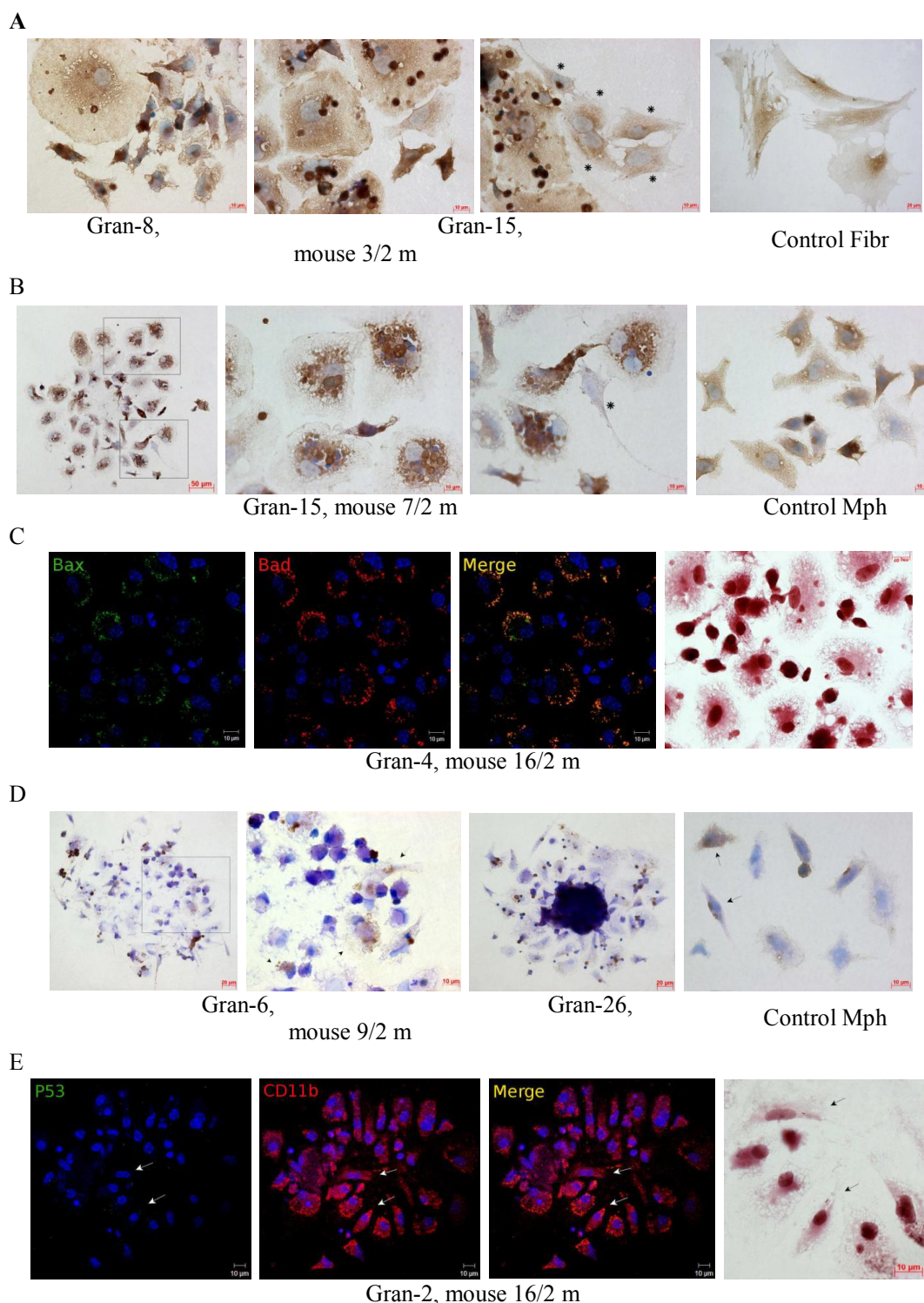


Figure 4: The cells with (A, C) Bax, (B-C) Bad, and (D-E) P53 proteins in the fragments of mouse splenic granulomas and control mouse peritoneal macrophages (Mph) and splenic fibroblasts (Fibr). The scale bars are (B, left panel) 50 μ m, ((A, right panel) and ((D, left and right central panels)) 20 μ m each, and (other panels) 10 μ m each. (A-B, D) The brown color indicates the presence of various antigens in the cells after immunochemical staining. (A-B) Black snowflakes indicate fibroblasts with the antigens. Other stained cells are macrophages, dendritic cells, and lymphocytes. The pictures of granuloma fragments (B, left and right central panels) are enlarged images of the areas defined by black boxes in picture (B, left panel). (D) A P53-positive macrophages are indicated by the black arrows. (C, E) Confocal immunofluorescent localization of the antigens in the cells. Colocalization of the markers on the confocal images of cells (yellow signal). Nuclei stained by DAPI (blue signal). In the right panels: the same fragments as in the other panels re-stained for acid-fast BCG mycobacteria by the ZN method. (C) The granuloma macrophages and dendritic cells without BCG mycobacteria, but with Bax (green signal) and Bad (red signal) proteins. (E) The granuloma macrophages with BCG mycobacteria and CD11b (red signal), but without P53 protein (green signal) are indicated by the white arrows on the fluorescent images and the black arrows on the ZN image.

mitochondrial pathway of apoptotic cell death [38,40]. The use of P53-specific antibodies did not reveal this antigen in the cytoplasm or nuclei of macrophages and dendritic cells, irrespective of the presence or absence of BCG mycobacteria in them, from the spleen granulomas of mice after one month and two months following infection with the BCG vaccine *in vivo* (Figures 4D, 4E and 5). Only a small number of control peritoneal macrophage cultures exhibited a background level of immunofluorescent staining for P53 protein, while most control and granuloma lymphocytes had this marker (Figures 4D and 5). P53 protein was not detected in granuloma fibroblasts or control lung and spleen fibroblasts. All granuloma platelet stained for P53 protein (Figure 4D). Thus, we have no evidence for whatever significant stabilization or accumulation of the P53 protein in the cytoplasm and nuclei of granuloma macrophages, dendritic cells and fibroblasts. Lack of P53 stabilization in granuloma cells, together with the unchanged morphology of their nuclei without evidence of chromatin condensation and nucleolar segregation, indicated that DNA in granuloma cells was undamaged and, consequently, the activators of this process were deficient. As is known [31,36], one of the main inducers of chromosome degradation, Apoptosis Inducing Factor (AIF), a flavoprotein with DNase functions, comes to the cell nuclei from the intermembrane space, where it normally occurs, only after pores have formed on the membrane of these organelles. It is therefore likely that the integrity of the mitochondrial outer membrane is preserved in mouse granuloma macrophages and dendritic cells, irrespective of the presence or absence of BCG mycobacteria in them.

Lack of activation of the executioner caspase-3 in mouse granuloma cells

As is known [62], caspase-3 is permanently present in cells as a non-active proenzyme; however, after its activation in the apoptosome, due to the release of apoptogenic factors from mitochondria, it becomes “executioner” and cleaves more than one hundred structural, signaling and regulatory proteins, making apoptosis inevitable. Consequently, caspase-3 activation is one of the main markers of apoptotic cell death. Cells were analyzed using antibodies that detect the active executioner form of caspase-3. Caspase-3 activation was detected in the cytoplasm of few macrophages, dendritic cell, fibroblasts and megakaryocytes of spleen granulomas obtained from mice after one month and two months following BCG infection *in vivo* (Figures 5 and 6). Cells aggregated within compacted granuloma structures did not have this marker (Figure 6). No caspase-3 activation was observed in control macrophage and fibroblast cultures (Figure 6). The presence of this marker in some granuloma lymphocytes, in most granuloma platelets and erythrocytes, as well as in the lymphocytes of control peritoneal macrophage cultures, could be accounted for not only by the apoptotic death of the cells, but also by their differentiation. As is known [63], caspase-3 activation is required for the formation of platelets and erythrocytes, and lymphocyte proliferation. On the whole, lack of caspase-3 activation in the mouse granuloma macrophages, dendritic cells and fibroblasts prevented their caspase-3-dependent apoptosis and was supposed to preserve the integrity of mitochondrial membranes in these cells.

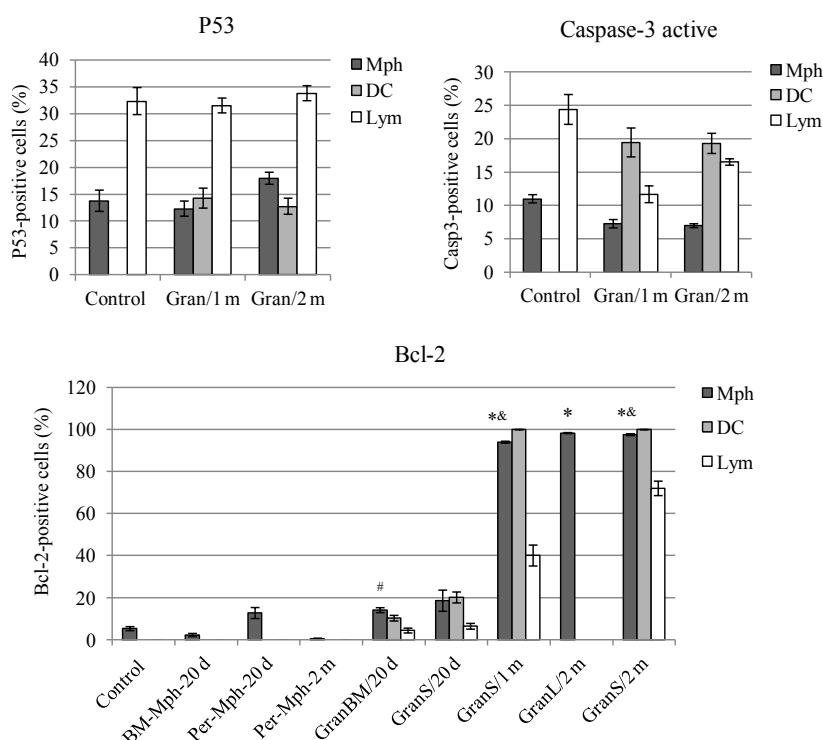
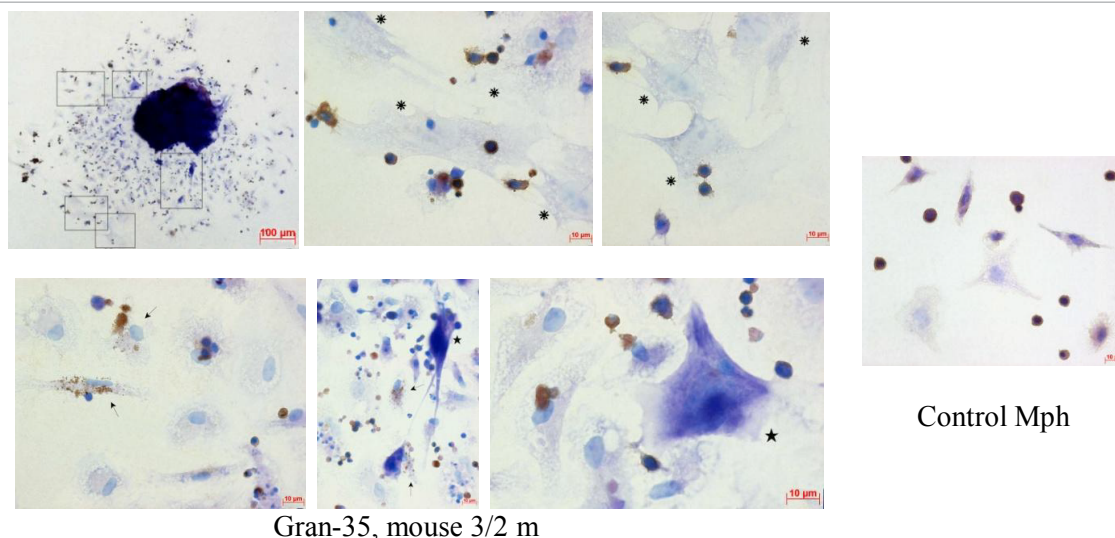


Figure 5: Macrophages (Mph), dendritic cells (DC), and lymphocytes (Lym) with P53, active caspase-3, and Bcl-2 proteins. The objects examined are control peritoneal macrophages from three intact mice (control), bone marrow and peritoneal macrophages obtained from two mice on 20 day following intraperitoneal infection with the BCG vaccine (BM-Mph-20 d and Per-Mph-20 d, respectively), peritoneal macrophages obtained from mouse 25 after two months following intraperitoneal infection with the BCG vaccine (Per-Mph-2 m), and granulomas from the bone marrow (BM/), lungs (L), and spleens (S) of two to five mice after 20 days (Gran/20 d), one month (Gran/1 m) and two months (Gran/2 m) following BCG infection *in vivo* and *ex vivo* culture for several hours. Gran/2 m granulomas of 12 mice were analyzed for Bcl-2. Granuloma cells producing various antigens were analyzed in each granuloma separately; the values were averaged all the mice and then combined for granulomas in each group. Data are expressed as the means \pm SEM. * $P < 0.001$ (comparisons of the number of Bcl-2-positive macrophages in Gran/1 m or Gran/2 m and control or Per-Mph-2 m); $^{\#}P < 0.01$ (comparisons of the number of Bcl-2-positive macrophages in GranS/1 m or GranS/2 m and GranS/20 d); $^{\&}P < 0.05$ (comparison of the number of Bcl-2-positive macrophages in GranBM/20 d and BM-Mph-20 d).



Gran-35, mouse 3/2 m

Control Mph

Figure 6: Immunohistochemical localization of the activation of caspase-3 in the cells of mouse splenic granuloma and control mouse peritoneal macrophages (Mph). The scale bars are (left upper panel) 100 µm and (other panels) 10 µm each. The pictures of granuloma fragments are enlarged images of the areas defined by black boxes in (a, left upper panel). The brown color indicates the presence of the antigen in these cells. Macrophages with active caspase-3 in them are indicated by the black arrows. The black stars and snowflakes indicate the megakaryocytes and fibroblasts, respectively that do not contain the antigen.

Thus, in granuloma cells with increased levels of the inducer of apoptosis TNF α , proapoptotic proteins Bax and Bad, death receptor Fas/CD95 and scavenger receptor CD36, we did not observe P53 stabilization or caspase-3 activation in macrophages and dendritic cells at the latent stage of BCG infection irrespective of the presence or absence of BCG mycobacteria in them. It is possible that the observed events of prevention of apoptotic death were most probably confined to times before mitochondrial and post-mitochondrial factors and effectors of apoptosis could spring to action and make changes irreversible.

The antiapoptotic protein Bcl-2 in granuloma cells from mice with latent tuberculous infection and in bone marrow and peritoneal macrophages after BCG infection *in vitro*

The Bcl-2 protein is one of the main factors that maintain due mitochondrial membrane permeability and protect cells from apoptosis [31,36]. Following immunohistochemical procedures, the cytoplasm of most macrophages, dendritic cells and megakaryocytes in lung and spleen granulomas obtained from mice after one month and two months following BCG infection *in vivo* for 2-5 days in *ex vivo* culture exhibited intense staining for Bcl-2 protein (Figures 5, 7A and 7B). However, much fewer macrophages of spleen and bone marrow granulomas had increased Bcl-2 protein after 20 days following BCG infection *in vivo* than at later times of latent tuberculous infection (Figures 5 and 7C). Nevertheless, there were more Bcl-2-positive macrophages in bone marrow granulomas than in the surrounding stroma (Figure 5). Control peritoneal macrophages as well as control lung and spleen fibroblasts did not stain for this marker (Figures 5, 7A and 7B). The number of lymphocytes with cytoplasmic Bcl-2 protein varied strongly between granulomas (Figures 5, 7A and 7B). No Bcl-2-positive lymphocytes were detected in control peritoneal macrophage cultures (Figures 5 and 7A). In the macrophages of bone marrow and peritoneal cell cultures infected with BCG *in vitro*, where increased mycobacterial loads and death of infected cells were observed throughout hours 72-120 of analysis [57], no induction of Bcl-2 synthesis was detected throughout hours 4-120 of analysis (Table 1 and Figure 7D). The number of Bcl-2-positive macrophages did not appear different between these cultures

Time*, h	Bcl-2-positive cells**, %			
	Bone marrow macrophages		Peritoneal macrophages	
	Control	BCG infection	Control	BCG infection
4	3.72 ± 1.66	1.76 ± 0.77	1.52 ± 0.74	0.75 ± 0.46
24	4.16 ± 1.04	3.49 ± 1.21	2.2 ± 0.96	2.61 ± 1.68
48	5.36 ± 2.29	1.39 ± 0.6	2.47 ± 1.75	2.38 ± 1.27
72	1.99 ± 0.6	3.9 ± 1.71	1.03 ± 0.62	0.67 ± 0.42
96	2.58 ± 1.27	2.34 ± 1.16	1.95 ± 1.42	2.85 ± 1.39
120	1.66 ± 0.94	2.72 ± 1.71	2.13 ± 1.37	2.64 ± 1.62

Table 1: Antiapoptotic protein Bcl-2 in mouse bone marrow and peritoneal macrophages infected with the BCG vaccine *in vitro* (BCG) or without infection (control) and after culture for as long as indicated.

and control bone marrow and peritoneal macrophages at the same times of analysis (data not shown).

Immunofluorescent visualization of the Bcl-2 antigen revealed not only a random pattern of staining of the cytoplasm of granuloma macrophages and fibroblasts, but also an intense staining of small roundish entities of varying size. These Bcl-2-positive entities were scattered throughout the cells and compacted granuloma structures as well as in the monolayer cultures of cells that had migrated from lung, spleen and bone marrow granulomas obtained from mice with latent tuberculous infection (Figures 7B,7C, and 8A-8D). Some Bcl-2-positive granuloma macrophages had acid-fast BCG mycobacteria in them, some did not (Figures 7B,7C, and 8A-8D). Some stand-alone entities that stained for Bcl-2 protein showed colocalization with the mitochondrial dye MitoTracker Deep Red FM in granuloma macrophages (Figure 7C). Bcl-2 protein was observed to partly colocalize with the proinflammatory cytokine TNF α (Figure 8A), the proapoptotic proteins Bax (Figure 8B), P53 (Figure 8C) and active caspase-3 (Figure 8D) in small roundish entities of varying size in mouse granuloma cells. Some granuloma macrophages and dendritic cells with large amounts of Bcl-2 protein had BCG mycobacteria in them, some did not (Figures 8C and 8D). Granuloma macrophages, whether with or without acid-fast BCG mycobacteria in them, largely exhibited a background level of immunofluorescent staining for P53 protein and active caspase-3 (Figures 8C and 8D). Thus, granulomas

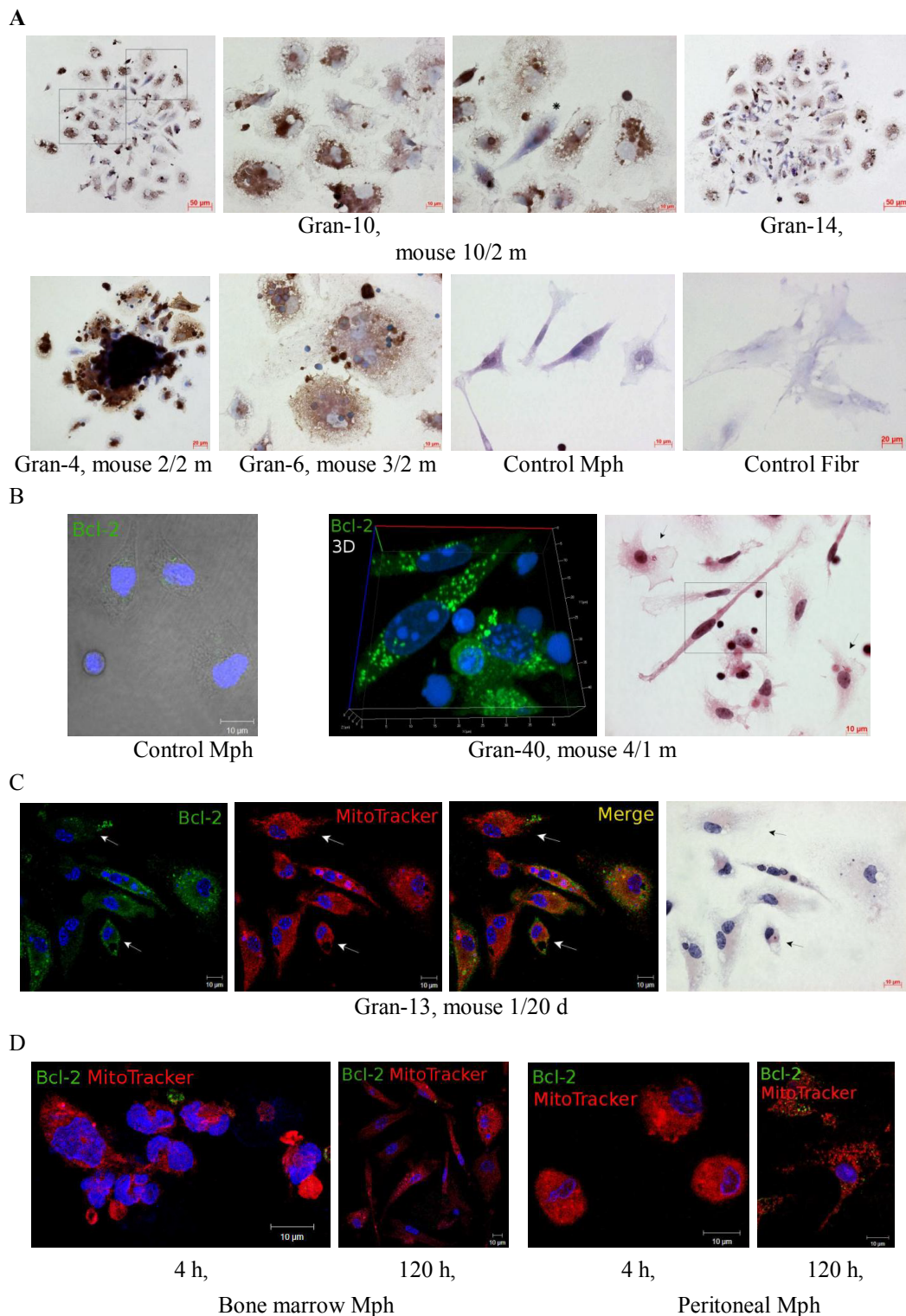


Figure 7: Antiapoptotic Bcl-2 protein in (A-C) the cells in the fragments of mouse splenic granulomas, control mouse peritoneal macrophages (Mph), splenic fibroblasts (Fibr), and (D) the bone marrow and peritoneal macrophages following infection with the BCG vaccine *in vitro* and after culture for several hours. The scale bars are (A, left and right upper panels) 50 μ m each, (A, left and right down panels) 20 μ m each, and (other panels) 10 μ m each. (A) The brown color indicates the presence of Bcl-2 protein in the cells after immunochemical staining. The pictures of granuloma fragments (A, left and right central top panels) are enlarged images of the areas defined by black boxes in picture (A, left top panel). (B-D) Confocal immunofluorescent localization of Bcl-2 protein (green signal) and MitoTracker Deep Red FM (red signal) in the cells. Colocalization of the markers on the confocal images of cells (yellow signal). Nuclei stained by DAPI (blue signal). (B) In the left panel: confocal image with phase contrast. (B-C) In the right panels: the same fragments as in the other panels re-stained for acid-fast BCG mycobacteria by the ZN method. A Bcl-2-producing macrophages with BCG mycobacteria are indicated by the white arrows on the fluorescent images and the black arrows on the ZN images.

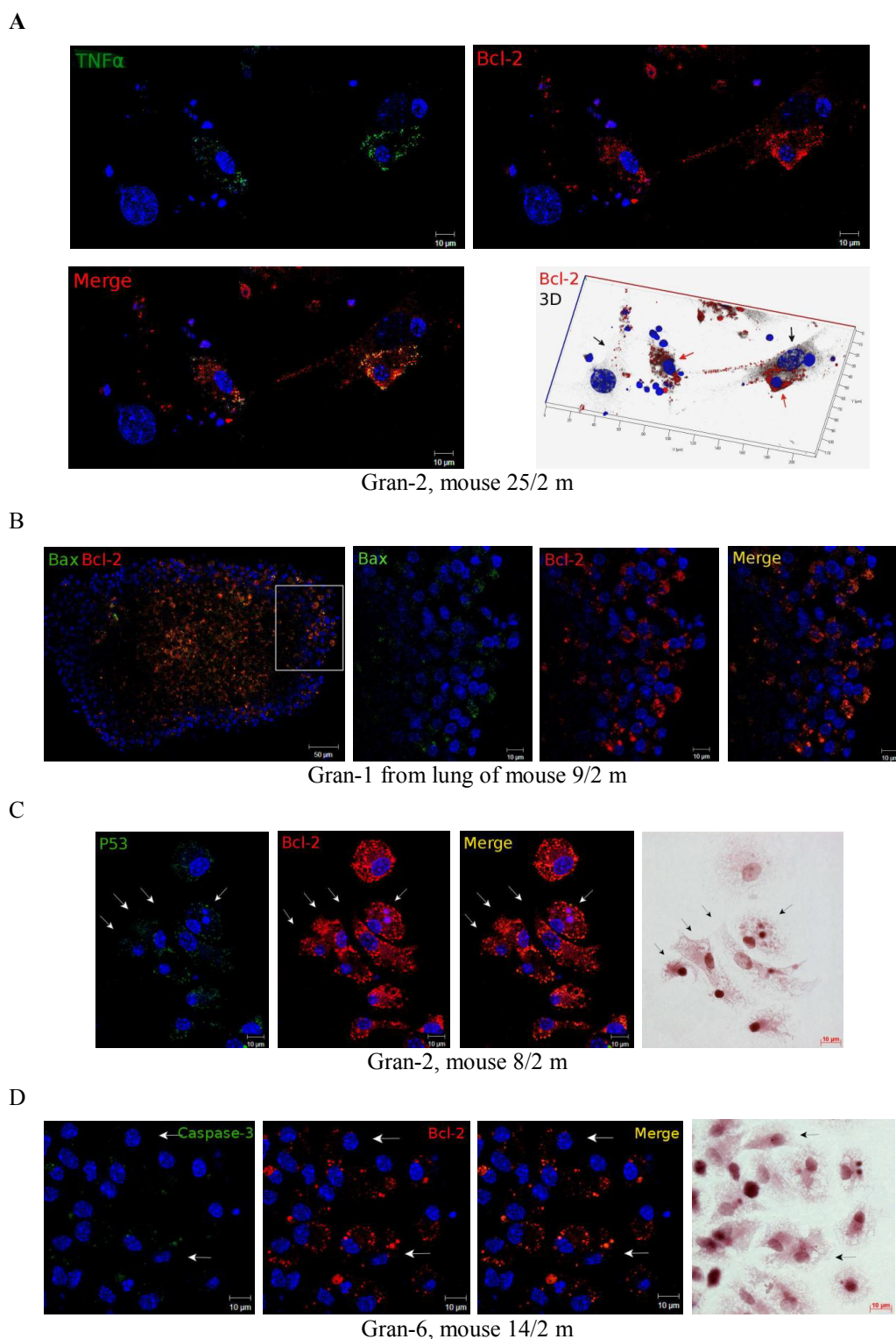


Figure 8: Representative confocal fluorescent images of macrophages stained by the Bcl-2-specific antibodies (red signal) and primary antibodies to (A) TNF α , (B) Bax, (C) P53, and (D) active caspase-3 (green signal) in (B) mouse lung granuloma and its fragment and (A, C-D) the fragments of mouse splenic granulomas. Colocalization of the markers on the confocal images of cells (yellow signal). Nuclei are stained by DAPI (blue signal). The scale bars are 10 μ m each. (A) Macrophages and fibroblasts with Bcl-2 protein are indicated by the red and black arrows on the 3D image (right down panel), respectively. (B) The pictures of granuloma fragment are enlarged images of the area defined by black boxes in picture (B, left panel). (C-D) In the right panels: the same fragments as in the other panels re-stained for acid-fast BCG mycobacteria by the ZN method. A Bcl-2-producing macrophages with BCG mycobacteria are indicated by the white arrows on the fluorescent images and the black arrows on the ZN images.

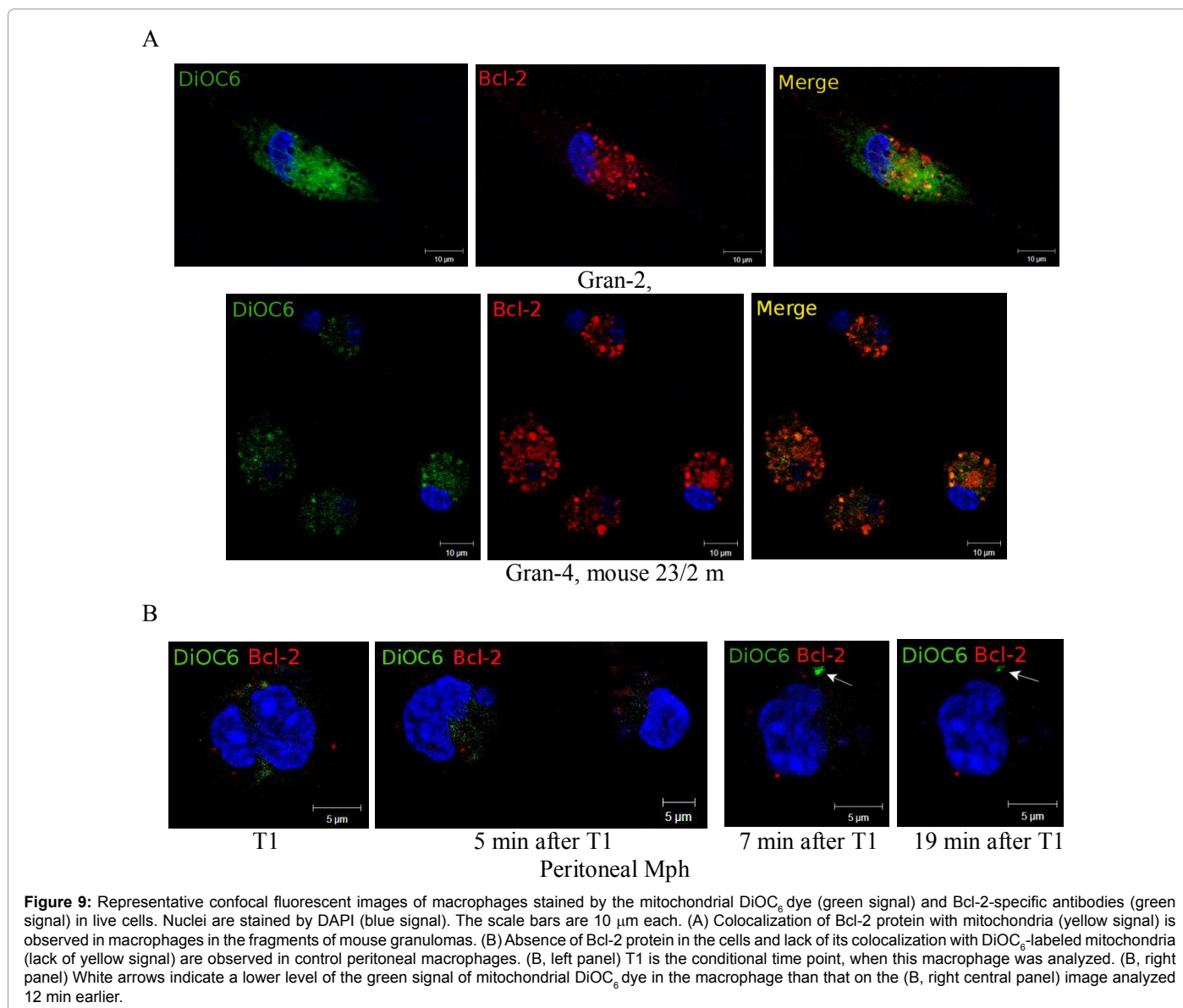
obtained from mice with latent tuberculous infection, especially at later times of its development, characteristically had increased the antiapoptotic protein Bcl-2 in different compartments of granuloma cells, including, probably, mitochondria, irrespective of the presence or absence of BCG mycobacteria in them.

Analysis of cells using the mitochondrial membrane potential-sensitive dye DiOC₆

The fluorescent lipophylic DiOC₆ is widely used on living cells in cytometric studies for analysis of mitochondrial depolarization, as decrease in the fluorescence intensity of this dye is regarded as an indicator of cell death [64]. We had previously observed an intense staining with DiOC₆ of roundish entities of varying size both in granuloma cells from mice with latent tuberculous infection and in control peritoneal macrophages and control lung and spleen fibroblasts (data not shown). In the present work, fluorescent living cell staining revealed the colocalization of the Bcl-2 protein and the DiOC₆ dye on small roundish entities of varying size scattered randomly throughout

the cytoplasm of granuloma macrophages from the spleen of mouse 23 following two months after BCG infection *in vivo* (Figure 9A). It is therefore quite likely that those stained cytoplasmic elements are mitochondria. Confocal microscopy performed immediately after this staining and fixation of granuloma cells revealed a gradual disappearance of the green signal, which was indicative of the presence of DiOC₆ in mitochondria, while the intensity of the red signal, which corresponded to the Bcl-2 protein, did not change. It is likely that we observed DiOC₆ migrating from mitochondria, with increasing mitochondrial depolarization and decreasing mitochondrial membrane potential ($\Delta\Psi_m$) in granuloma cell killed by fixation. We also note that even though the living cell staining procedure was quite long, the morphology of granuloma macrophages remained unaffected: no nuclear fragmentation was observed; mitochondria occurring throughout the cells were comparable in size with those previously detected by staining for Bcl-2 protein and MitoTracker Deep Red FM together (Figures 7C and 8A).

Confocal microscopy of the results of two similar experiments with



the staining of peritoneal macrophages not infected *in vitro* revealed immediately proapoptotic changes in cell morphology, lack of staining for Bcl-2 protein and a minimum DiOC₆ fluorescence (Figure 9B). We observed nuclear fragmentation in peritoneal macrophages, typical of apoptotic cell death, and rapidly vanishing dot-sized DiOC₆ signals in perinuclear regions (Figure 9B). We note that control peritoneal macrophages that were not exposed to staining had no morphological signs of cell death *in vitro* (data not shown). It is possible that the living cell staining procedures, which adversely affect cell viability, were long enough to allow control macrophages to die rapidly, with their nuclei fragmented, spatially oriented mitochondrial network ruined, and organelles translocating to the nuclear region. In contrast to granuloma macrophages, control peritoneal macrophages stained very little for Bcl-2 protein (Figure 9B), and so did other control cultures (Figures 5, 7A and 7B). Thus, control peritoneal macrophages did not have Bcl-2 protein and, therefore, could not prevent the leak of factors and inducers of apoptotic cell death from mitochondria. The observed dotted pattern of cell staining with DiOC₆ (Figure 9B) suggested reduced mitochondrial $\Delta\Psi_m$ in the control peritoneal macrophages and was yet another hallmark of their apoptotic death.

It was previously established [56] that one-third of macrophages in granulomas from the spleen of mouse 23 after two months following BCG infection *in vivo* had a considerable number of acid-fast BCG mycobacteria in them, including as growing colonies with the cord morphology (the indicator of mycobacterial virulence). However, mouse 23 granuloma macrophages that stained intensely for the antiapoptotic protein Bcl-2 did not have morphological signs of apoptotic or necrotic death (Figure 9A). Consequently, the Bcl-2 protein, which was observed in large amounts in the cytoplasm and, probably, mitochondria of macrophages in mouse 23 granulomas, can be regarded as one of the factors that protected granuloma cells from death both during long live cell staining procedures in *ex vivo* culture and, probably, *in vivo*, in granulomas containing large numbers of BCG-infected cells.

Together, the results obtained suggest that the antiapoptotic protein Bcl-2 promoted the viability of granulomas' macrophages and other cell types, irrespective of the presence or absence of BCG mycobacteria in them, not only in *ex vivo* culture or during live cell staining, but also in the animal organisms under a considerable amount of pressure from mycobacterial, proinflammatory and proapoptotic factors in granulomatous inflammatory lesions at different times of latent tuberculous infection in mice.

Discussion

Apoptotic death of cells infected with mycobacteria is considered to be one of the main mechanisms by which an affected organism can withstand tuberculous infection [4,5,7-9,24,25]. Apoptosis leads not only to disposal of digested apoptotic cells with mycobacteria and their elimination in phagosomes, but also to an efficient processing of mycobacterial antigens used by antigen-presenting cells for the maintenance and enhancement of the immune response to the pathogen [24]. It has been established that *in vitro* infection of different cell types with non-virulent strains of mycobacteria led these cells to rapid death by TNF α -induced receptor-dependent apoptosis [48,52,65]. However, our previous studies using the *ex vivo* model of granulomatous inflammatory lesions in mice did not reveal, at any time of latent tuberculous infection, morphological signs of apoptotic or necrotic death in granuloma macrophages or dendritic cells differently loaded with mycobacteria of the attenuated BCG strain [55-57].

Now, analysis of the expression of the markers of the development/abrogation of apoptosis demonstrated increased levels of the inducer of apoptosis TNF α , proapoptotic proteins Bax and Bad, death receptor Fas/CD95 and scavenger receptor CD36 in the cells of granulomas obtained from the spleens, lungs and bone marrow of BCG-infected mice at different times of latent tuberculous infection. However, we did not observe any significant stabilization of the P53 protein or activation of the major executioner caspase-3 in the cytoplasm and nuclei of granuloma macrophages, dendritic cells, fibroblasts and megakaryocytes. At the same time, the antiapoptotic protein Bcl-2 was in large amounts observed in the cytoplasm and mitochondria of granuloma cells, especially at later times of latent tuberculous infection.

As is known, the Bcl-2 protein, which occurs on the mitochondrial outer membrane, interferes with pore formation and the release of proapoptotic cytochrome *c* and AIF from mitochondrial intermembrane space, and thus prevents activation of caspases, nuclear DNA degradation and apoptosis [36]. Also, Bcl-2 protein is acted on by activated caspase-3 and the Bax and P53 proteins, which abrogates its antiapoptotic functions [31,36,64]. The observed colocalization of the protein Bcl-2 with the proapoptotic proteins Bax and P53 and active caspase-3 on the mitochondria of granuloma cells suggests that they interacted with one another on these organelles in mouse granuloma cells. No colocalization of Bcl-2 protein with Bax protein was observed in the cytoplasm of granuloma cells. This observation is in agreement with studies of Edlich et al. [66,67], who found that non-active Bax protein is continuously recycling in the cells between the cytoplasm and mitochondria, while, on the mitochondrial outer membrane, non-active Bax protein directly interacts with the antiapoptotic proteins Bcl-2 and Bcl-x_L and then returns to the cytoplasm with their assistance. In the cytoplasm, Bax protein immediately dissociates from the complex assembled on mitochondria. It was demonstrated [66,67] that the balance between mitochondrial and cytosolic Bax protein can additionally be regulated by BH3-domain-containing proteins, including Bad, which promotes activation of Bax protein in their complex on the mitochondrial outer membrane, by the formation of pores and increase in their permeability, as well as by disabling Bax recycling in the cells. In mouse granuloma cells, we observed the proapoptotic proteins Bad and Bax colocalizing, probably on the mitochondrial outer membrane, and the activation of this complex. However, the accumulation of the potential-sensitive dye DiOC₆ in granuloma macrophage mitochondria suggested that their membranes were intact and that $\Delta\Psi_m$ was preserved. We proposed that the protection of the mitochondria of granuloma cells from proapoptotic factors depends on Bcl-2 protein, which was found in large amounts in the cytoplasm and mitochondria of granuloma cells. As is known [30,36,61], elevated Bcl-2 protein on the mitochondrial membranes interferes with pore formation due to the action of the proapoptotic proteins Bax and Bad, stabilizes these organelles and abrogates apoptotic dying. For example, overexpression of Bcl-2 protein contained within an expression vector introduced to mouse L929 fibrosarcoma cells protected these cells from death, which was promoted by the inducer of apoptosis TNF α , and the mitochondria of these cells had increased $\Delta\Psi_m$ [68]. Because $\Delta\Psi_m$ and the proton gradient on the mitochondrial inner membrane are the main sources of energy for ATP synthesis, reduction in $\Delta\Psi_m$, which is normally associated with the opening of non-selective pores, is catastrophic for cellular respiration and energy-related processes in the cell and, eventually, fatal for these cells [69]. Preservation of mitochondrial $\Delta\Psi_m$ during staining of living granuloma macrophages containing large amounts of the Bcl-2 protein was indicative of its involvement in maintaining the integrity of mitochondrial elements and the protection

of granuloma cells from death, because in similar experiments the control macrophages that did not have any Bcl-2 protein in them had considerably reduced $\Delta\Psi_m$ and exhibited morphological signs of apoptotic death.

In addition to protecting cells from apoptosis, Bcl-2 protein can protect mammalian cells from autophagy by interacting with the BH3-like domain of the Beclin-1 protein and abrogating its functions in the formation of autophagosomal membranes [70]. It was established [70] that an essential role in preventing autophagy should be given to the Bcl-2 protein that is located on the endoplasmic reticulum, not to that on mitochondrial membranes. In our experiments, not only the mitochondria of granuloma macrophages and dendritic cells stained intensely for Bcl-2 protein, irrespective of the presence or absence of acid-fast BCG mycobacteria in them, but also the cytoplasm near the nucleus, where the endoplasmic reticulum basically occurs. Whether Bcl-2 protein is involved in the regulation of autophagy in the granuloma cells of mice at the latent stage of tuberculous infection remains to be known.

The observed increased Bcl-2 levels in most mouse granuloma cells poses the question about the life cycle of this protein in these cells. The half-life of Bcl-2 protein in cells is 24 h on average [70]. In human follicular lymphoma cells, where the gene encoding this protein was originally identified, the t(14;18) chromosomal rearrangement is often [71]. Following this rearrangement, the Bcl-2 encoding gene is acted on by the activated enhancers of genes for immunoglobulin heavy chains and, consequently, is continuously transcribed, which leads to cellular accumulation of Bcl-2 protein and its mRNA. As a result, lymphocytes lose sensitivity to proapoptotic stimuli, which leads to lymphomas. A mechanism of Bcl-2 accumulation like this is unlikely to operate in mouse granuloma cells, because macrophages and dendritic cells are highly differentiated and do not divide, nor is it likely that this rearrangement may occur in many cells at once. Other mechanisms of cellular Bcl-2 accumulation imply its post-translational modifications, which allow ubiquitination and proteasomal degradation to be escaped. It has been demonstrated [72] that phosphorylation of particular serine and threonine residues protected Bcl-2 protein from degradation and promoted its accumulation in different cell types, while dephosphorylation of these residues by the proinflammatory cytokine TNF α led to the destruction of proteasomal Bcl-2 and apoptosis without any change in Bcl-2 mRNA levels. Furthermore, it has been found [73] that nitrosylation of cysteine residues of Bcl-2 protein by endogenous nitric oxide abrogated its proteasomal degradation and protected cells from apoptotic death. Increased Bcl-2 protein in nucleus-free platelets of the mouse granulomas studied was suggestive of post-translational mechanisms of its stabilization in this cell type. At the same time, increased TNF α production in granuloma macrophages and dendritic cells was indicative of activation of the synthesis and/or maintenance of Bcl-2 mRNA with its continuous *de novo* production in granuloma cells. It is also known [64] that Bcl-2 protein located in different cellular compartments can be regulated differently. For example, in human peripheral blood T lymphocytes, mitochondrial Bcl-2 protein had reduced stability—in contrast to Bcl-2 protein on the nuclear envelope [64]. It is also known [76] that the proinflammatory cytokines TNF α and IL-1, an increased production of which was observed in granulomas from BCG-infected mice [55,57], can, through the links with their receptors, activate the transcription factor NF- κ B, which induces expression of the *bcl-2* gene. Thus, regulation of Bcl-2 levels in different cell types is complex and can be exerted from different layers by a variety of mechanisms. Therefore, further analysis of the ways in which Bcl-2 levels are regulated in the granuloma cells of mice with latent tuberculous infection is required.

Meanwhile, we asked ourselves if increased Bcl-2 protein has relevance to the presence of BCG mycobacteria in the macrophages or it is simply part of the regular proinflammatory response of the host's cells to intracellular microbial infection in granulomatous inflammatory lesions. In a study of Mogga et al. [74], it was not before week 16 following infection of mice with the virulent strain H37Rv of *M. tuberculosis* intraperitoneally that Bcl-2 protein became detectable by immunohistochemistry in lung tissue cells (about 5% of cells studied) that stained for mycobacterial antigens—but not for Bax protein. Natarajan and Sujatha observed a twofold increase in Bcl-2 levels as early as 24 h after *in vitro* infection of THP-1 monocyte-like cells with the virulent strain H37Rv of *M. tuberculosis* [52]. By contrast, blood mononuclear cells and human THP-1 cells infected *in vitro* with attenuated BCG mycobacteria or non-virulent *M. tuberculosis* strain H37Ra had a considerable reduction in Bcl-2 protein after 24 h following infection [52,75]. We did not observe activation of Bcl-2 synthesis at hours 4-120 of analysis in the macrophages from bone marrow cell cultures and peritoneal exudates infected with BCG mycobacteria *in vitro*. At the same time, we observed increased mycobacterial loads and death of cells at hours 72-120 of analysis [57]. The granulomas studied had different numbers of infected cells, including macrophages and dendritic cells, from the lowest, as in mouse 25 after two months following BCG infection *in vivo*, to the highest, as in mice 14, 16, 21, and 23 after two months following BCG infection *in vivo*; some of the granulomas did not have any infected cells in them at all [56]. However, all granulomas studied from mice after one month and two months following infection with the BCG vaccine *in vivo* had increased Bcl-2 virtually in all macrophages and dendritic cells, irrespective of the presence or absence of acid-fast BCG mycobacteria in them. High Bcl-2 levels were also observed in all granuloma fibroblasts, megakaryocytes, platelets and some granuloma lymphocytes. However, peritoneal macrophages isolated in parallel with granuloma cells from mouse 25 two months following intraperitoneal infection did not stain for Bcl-2 protein. This protein was detected only in a small number of the macrophages and dendritic cells of macrophages obtained from mice after 20 days following infection with the BCG vaccine *in vivo*. However, the number of Bcl-2-positive macrophages was significantly higher in bone marrow granuloma than in the surrounding stroma. Consequently, high Bcl-2 levels appear to be a feature of granuloma cells, especially as latent tuberculous infection in mice becomes chronic (one month and two months following infection with the BCG vaccine *in vivo*) in the presence of mycobacterial, proinflammatory and proapoptotic factors in granulomatous inflammatory lesions. Bcl-2 production in mouse granuloma cells appears to be induced and maintained irrespective of the presence or absence of BCG mycobacteria in them. It is possible that the antiapoptotic protein Bcl-2 acts to protect granulomas as a whole and their individual cells from death, including those heavily infected with BCG mycobacteria. As a result, Bcl-2-positive granuloma macrophages with large numbers of BCG mycobacteria in them were viable and did not have a characteristic apoptotic or necrotic morphology, while Bcl-2-negative macrophages heavily loaded with BCG mycobacteria in the different cultures of mouse cells following BCG infection *in vitro* had increased death rates [57]. As was proposed [77], the apoptotic death of macrophages infected with mycobacteria *in vivo* should not necessarily be good for the organism, because the elimination of the cells that have been activated by mycobacteria leads to the weakening of the overall microbicidal response to infection, which, in turn, helps the pathogen survive and evade the host's immunity. It is possible that it was BCG infection of mice *in vivo* that triggered not only the formation of granulomatous inflammatory lesions in the organs and tissues, but also the development of protective reactions of cells, including by

increasing their levels of the antiapoptotic protein Bcl-2. Whether this event is specific for the granulomas that were induced by mycobacterial infection or it is typical of granulomatous inflammatory lesions of non-infectious origin remains to be known.

Note that the proinflammatory cytokine TNF α , the production of which was induced following exposure to BCG infection both *in vivo* and *in vitro*, may have contrasting effects on the infected organism. As is known [2-4,9,19,34], TNF α -induced apoptosis of infected cells considerably reduces the bacterial load. However, overexpression of TNF α protein leads to the development of an uncontrollable inflammatory response in tissues and organs, which can result in the clinical signs of tuberculosis in man [2-4,34]. Therefore, proper regulation of the proinflammatory and costimulating activities of TNF α protein, as well as its proapoptotic effects depending on various factors acting on the cells in granulomatous inflammatory lesions is of major importance. An outstanding role in this choice should be given to granuloma cells' receptors, which can act pleiotropically. For example, activation of the costimulating molecule CD30, a member of the TNF α receptor superfamily, on the cell membrane, on the one hand, had an antiapoptotic effect on T and B lymphocytes; while, on the other hand, activated, via its signaling pathways, expression of the gene for the death receptor Fas/CD95 [58]. Overall, it is possible that the involvement of different receptors, which occur on the cell membrane and induce different signaling pathways helps exert a fine-tuned regulation on TNF α activity on granuloma cells and promote either their survival or their death in the granulomatous inflammatory lesions in mice at various times of latent tuberculous infection.

Conclusions

This study of granulomas from mice with latent tuberculous infection using an *ex vivo* model did not reveal activation of proteins involved in the irreversible development of apoptotic death of granuloma cells irrespective of the presence or absence of BCG mycobacteria in them – not even in the presence of a large number of proapoptotic stimuli and factors. The antiapoptotic protein Bcl-2, found in large amounts in the cytoplasm and, probably, mitochondria of granuloma cells, irrespective of the presence or absence of mycobacteria in them, may have probably been involved in the maintenance of their viability endangered by mycobacterial, proinflammatory and proapoptotic factors in mouse granulomatous inflammatory lesions. Overall, the importance of analysis of intercellular and intracellular relationships between various inducers, effectors and suppressors of cell death, which influence the survival of cell with mycobacteria in the granulomatous inflammatory lesions of animals with latent tuberculous infection, is unquestionable. These interactions can result either in activation of infection into an acute tuberculous process or in a long symptom-free latent stage, which may either end up destroying all mycobacteria or last for even longer and keep mycobacteria persisting in the cells of the host organism.

Conflict of Interests

The author declares that no conflict of interests exists.

Acknowledgments

The author is thankful to Dr. S.I. Baiborodin and T.E. Aleshina of the Shared Center for Microscopic Analysis of Biological Objects of the Institute of Cytology and Genetics, for technical support; Professor L.E. Panin of the Research Institute of Biochemistry, for support to this work and helpful discussion.

References

1. Lawn SD, Zumla AI (2011) Tuberculosis. *Lancet* 378: 57-72.
2. Sasindran SJ, Torrelles JB (2011) Mycobacterium tuberculosis infection and

inflammation: what is beneficial for the host and for the bacterium? *Front Microbiol* 2: 1-16.

3. Cheallaigh CN, de Castro CP, Coleman MM, Hope JC, Harris J (2012) Macrophages and tuberculosis. In: *Handbook of Macrophage*, Nova Science Publisher, New York.
4. Espitia C, Rodríguez E, Raman-Luing L, Echeverría-Valencia G, Vallecillo AJ (2012) Host-pathogen interactions in tuberculosis. In: *Understanding Tuberculosis - Analyzing the Origin of Mycobacterium Tuberculosis Pathogenicity*. In Tech, Vienna.
5. Xu G, Wang J, Gao GF, Liu CH (2014) Insights into battles between Mycobacterium tuberculosis and macrophages. *Protein Cell* 5: 728-736.
6. Prendergast KA, Kirman JR (2013) Dendritic cell subsets in mycobacterial infection: control of bacterial growth and T cell responses. *Tuberculosis* 93:115-122.
7. Srivastava S, Ernst JD, Desvignes L (2014) Beyond macrophages: the diversity of mononuclear cells in tuberculosis. *Immunol Rev* 262: 179-192.
8. Hmama Z, Peña-Díaz S, Joseph S, Av-Gay Y (2015) Immuno-evasion and immunosuppression of the macrophage by Mycobacterium tuberculosis. *Immunol Rev* 264: 220-232.
9. Weiss G, Schaible UE (2015) Macrophage defense mechanisms against intracellular bacteria. *Immunol Rev* 264:182-203.
10. Pieters J (2008) Mycobacterium tuberculosis and the macrophage: maintaining a balance. *Cell Host Microbe* 3: 399-407.
11. Ahmad S (2011) Pathogenesis, immunology, and diagnosis of latent Mycobacterium tuberculosis infection. *Clin Dev Immunol* 814943.
12. Flynn JL, Chan J, Lin PL (2011) Macrophages and control of granulomatous inflammation in tuberculosis. *Mucosal Immunol* 4: 271-278.
13. Vergne I, Chua J, Deretic V (2003) Mycobacterium tuberculosis phagosome maturation arrest: selective targeting of PI3P-dependent membrane trafficking. *Traffic* 4: 600-606.
14. Vergne I, Chua J, Singh SB, Deretic V (2004) Cell biology of mycobacterium tuberculosis phagosome. *Annu Rev Cell Dev Biol* 20: 367-394.
15. Deretic V, Singh S, Master S, Harris J, Roberts E, et al. (2006) Mycobacterium tuberculosis inhibition of phagolysosome biogenesis and autophagy as a host defence mechanism. *Cell Microbiol* 8: 719-727.
16. Ehrh S, Schnappinger D (2009) Mycobacterial survival strategies in the phagosome: defence against host stresses. *Cell Microbiol* 11: 1170-1178.
17. Meena LS, Rajni (2010) Survival mechanisms of pathogenic Mycobacterium tuberculosis H37Rv. *FEBS J* 277: 2416-2427.
18. Seto S, Tsujimura K, Koide Y (2011) Rab GTPases regulating phagosome maturation are differentially recruited to mycobacterial phagosomes. *Traffic* 12: 407-420.
19. Cooper AM, Mayer-Barber KD, Sher A (2011) Role of innate cytokines in mycobacterial infection. *Mucosal Immunol* 4: 252-260.
20. Redford PS, Murray PJ, O'Garra A (2011) The role of IL-10 in immune regulation during M. tuberculosis infection. *Mucosal Immunol* 4: 261-270.
21. Quesniaux V, Garcia I, Jacobs M, Ryffel B (2012) Role of TNF in host resistance to tuberculosis infection: membrane TNF is sufficient to control acute infection. In: *Understanding Tuberculosis - Analyzing the Origin of Mycobacterium Tuberculosis Pathogenicity*. InTech, Vienna.
22. Kornfeld H, Mancino G, Colizzi V (1999) The role of macrophage cell death in tuberculosis. *Cell Death Differ* 6: 71-78.
23. Lamkanfi M, Dixit VM (2010) Manipulation of host cell death pathways during microbial infections. *Cell Host Microbe* 8: 44-54.
24. Behar SM, Martin CJ, Booty MG, Nishimura T, Zhao X, et al. (2011) Apoptosis is an innate defense function of macrophages against Mycobacterium tuberculosis. *Mucosal Immunol* 4: 279-287.
25. Lee J, Hartman M, Kornfeld H (2009) Macrophage apoptosis in tuberculosis. *Yonsei Med J* 50: 1-11.
26. Fairbairn IP (2004) Macrophage apoptosis in host immunity to mycobacterial infections. *Biochem Soc Trans* 32: 496-498.

27. Clay H, Volkman HE, Ramakrishnan L (2008) Tumor necrosis factor signaling mediates resistance to mycobacteria by inhibiting bacterial growth and macrophage death. *Immunity* 29: 283-294.
28. Davis JM, Ramakrishnan L (2009) The role of the granuloma in expansion and dissemination of early tuberculous infection. *Cell* 136: 37-49.
29. Gutierrez MG, Master SS, Singh SB, Taylor GA, Colombo MI, et al. (2004) Autophagy is a defense mechanism inhibiting BCG and Mycobacterium tuberculosis survival in infected macrophages. *Cell* 119: 753-766.
30. Espert L, Beaumelle B, Vergne I (2015) Autophagy in Mycobacterium tuberculosis and HIV infections. *Front Cell Infect Microbiol* 5: 49.
31. Porter AG (1999) Protein translocation in apoptosis. *Trends Cell Biol* 9: 394-401.
32. Martelli AM, Zweyer M, Ochs RL, Tazzari PL, Tabellini G, et al. (2001) Nuclear apoptotic changes: an overview. *J Cell Biochem* 82: 634-646.
33. Shen HM, Pervaiz S (2006) TNF receptor superfamily-induced cell death: redox-dependent execution. *FASEB J* 20:1589-1598.
34. Mootoo A, Stylianou E, Arias MA, Reljic R (2009) TNF- α in tuberculosis: a cytokine with a split personality. *Inflamm Allergy Drug Targets* 8: 53-62.
35. Tran TM, Temkin V, Shi B, Pagliari L, Daniel S, et al. (2009) TNF α -induced macrophage death via caspase-dependent and independent pathways. *Apoptosis* 14: 320-332.
36. Van Loo G, Saelens X, van Gurp M, MacFarlane M, Martin SJ, et al. (2002) The role of mitochondrial factors in apoptosis: a Russian roulette with more than one bullet. *Cell Death Differ* 9: 1031-1042.
37. Marine JC, Lozano G (2010) Mdm2-mediated ubiquitylation: p53 and beyond. *Cell Death Differ* 17: 93-102.
38. Haupt S, Berger M, Goldberg Z, Haupt Y (2003) Apoptosis - the p53 network. *J Cell Sci* 116: 4077-4085.
39. Chipuk JE, Kuwana T, Bouchier-Hayes L, Droin NM, Newmeyer DD, et al. (2004) Direct activation of Bax by p53 mediates mitochondrial membrane permeabilization and apoptosis. *Science* 303: 1010-1014.
40. Chari NS, Pinaire NL, Thorpe L, Medeiros LJ, Routbort MJ, et al. (2009) The p53 tumor suppressor network in cancer and the therapeutic modulation of cell death. *Apoptosis* 14: 336-347.
41. Biton S, Ashkenazi A (2011) NEMO and RIP1 control cell fate in response to extensive DNA damage via TNF- α feedforward signaling. *Cell* 145: 92-103.
42. Saunders BM, Britton WJ (2007) Life and death in the granuloma: immunopathology of tuberculosis. *Immunol Cell Biol* 85: 103-111.
43. Mohan VP, Scanga CA, Yu K, Scott HM, Tanaka KE, et al. (2001) Effects of tumor necrosis factor alpha on host immune response in chronic persistent tuberculosis: possible role for limiting pathology. *Infect Immun* 69: 1847-1855.
44. Harris J, Keane J (2010) How tumour necrosis factor blockers interfere with tuberculosis immunity. *Clin Exp Immunol* 161: 1-9.
45. Keane J, Remold HG, Kornfeld H (2000) Virulent Mycobacterium tuberculosis strains evade apoptosis of infected alveolar macrophages. *J Immunol* 164: 2016-2020.
46. O'Sullivan MP, O'Leary S, Kelly DM, Keane J (2007) A caspase-independent pathway mediates macrophages cell death in response to Mycobacterium tuberculosis infection. *Infect Immun* 75: 1984-1993.
47. van der Wel N, Hava D, Houben D, Fluitsma D, van Zon M, et al. (2007) M. tuberculosis and M. leprae translocate from the phagolysosome to the cytosol in myeloid cells. *Cell* 129: 1287-1298.
48. Abebe M, Kim L, Rook G, Aseffa A, Wassie L, et al. (2011) Modulation of cell death by M. tuberculosis as a strategy for pathogen survival. *Clin Dev Immunol* 2011: 678570.
49. Sly LM, Hingley-Wilson SM, Reiner NE, McMaster WR (2003) Survival of Mycobacterium tuberculosis in host macrophages involves resistance to apoptosis dependent upon induction of antiapoptotic Bcl-2 family member Mcl-1. *J Immunol* 170: 430-437.
50. Falcone V, Basse EB, Toniolo A, Conaldi PG, Collins FM (1994) Differential release of tumor necrosis factor- α from murine peritoneal macrophages stimulated with virulent and avirulent species of mycobacteria. *FEMS Immunol Med Microbiol* 8: 225-232.
51. Roach DR, Bean AGD, Demangel C, France MP, Briscoe H, et al. (2002) TNF regulates chemokine induction essential for cell recruitment, granuloma formation, and clearance of mycobacterial infection. *J Immunol* 168: 4620-4627.
52. Natarajan PL, Sujatha N (2011) Mitogen-activated protein kinases mediate the production of B-cell lymphoma 2 protein by Mycobacterium tuberculosis monocytes. *Biochemistry (Moscow)* 76: 938-950.
53. Clay H, Davis J, Beery D, Huttenlocher AS, Lyons S, et al. (2007) Dichotomous role of the macrophage in early Mycobacterium marinum infection of the zebrafish. *Cell Host Microbe* 2: 29-39.
54. Egen JG, Rothfuchs AG, Feng CG, Winter N, Sher A, et al. (2008) Macrophage and T cell dynamics during the development and disintegration of mycobacterial granulomas. *Immunity* 28: 271-284.
55. Ufimtseva E (2013) Investigation of functional activity of cells in granulomatous inflammatory lesions from mice with latent tuberculous infection in the new ex vivo model. *Clin Dev Immunol* 371249.
56. Ufimtseva E (2015) Mycobacterium-Host Cell Relationships in Granulomatous Lesions in a Mouse Model of Latent Tuberculous Infection. *Biomed Res Int* 948131.
57. Ufimtseva E (2016) Differences between Mycobacterium-host cell relationships in latent tuberculous infection of mice ex vivo and mycobacterial infection of mouse cells in vitro. *J Immunol Res* 4325646.
58. Muta H, Boise LH, Podack ER (2000) CD30 signals integrate expression of cytotoxic effector molecules, lymphocyte trafficking signals, and signals for proliferation and apoptosis. *J Immunol* 165: 5105-5111.
59. Febbraio M, Hajjar DP, Silverstein RL (2001) CD36: a class B scavenger receptor involved in angiogenesis, atherosclerosis, inflammation, and lipid metabolism. *J Clin Invest* 108: 785-791.
60. Deutsch VR, Tomer A (2006) Megakaryocyte development and platelet production. *Br J Haematol* 134: 453-466.
61. Gogvadze V, Orrenius S, Zhivotovsky B (2009) Mitochondria as targets for chemotherapy. *Apoptosis* 14: 624-640.
62. Köhler C, Orrenius S, Zhivotovsky B (2002) Evaluation of caspase activity in apoptotic cells. *J Immunol Methods* 265: 97-110.
63. Nhan TQ, Liles WC, Schwartz SM (2006) Physiological functions of caspases beyond cell death. *Am J Pathol* 169: 729-737.
64. Scheel-Toellner D, Raza K, Assi L, Pilling D, Ross EJ, et al. (2008) Differential regulation of nuclear and mitochondrial Bcl-2 in T cell apoptosis. *Apoptosis* 13: 109-117.
65. Song CH, Lee J-S, Lee S-H, Lim K, Kim H-J, et al. (2003) Role of mitogen-activated protein kinase pathways in the production of tumor necrosis factor- α , interleukin-10, and monocyte chemoattractant protein-1 by Mycobacterium tuberculosis H37Rv-infected human monocytes. *J Clin Immunol* 23: 194-201.
66. Edlich F, Banerjee S, Suzuki M, Cleland MM, Arnoult D, et al. (2011) Bcl-x(L) retrotranslocates Bax from the mitochondria into the cytosol. *Cell* 145: 104-116.
67. Todt F, Cakir Z, Reichenbach F, Emschermann F, Lauterwasser J, et al. (2015) Differential retrotranslocation of mitochondrial Bax and Bak. *EMBO J* 34: 67-80.
68. Hennes T, Bertoni G, Richter C, Peterhans E (1993) Expression of BCL-2 protein enhances the survival of mouse fibrosarcoma cells in tumor necrosis factor-mediated cytotoxicity. *Cancer Res* 53: 1456-1460.
69. Bras M, Queenan B, Susin SA (2005) Programmed cell death via mitochondria: different modes of dying. *Biochemistry (Mosc)* 70: 231-239.
70. Patingre S, Tassa A, Qu X, Garuti R, Liang XH, et al. (2005) Bcl-2 antiapoptotic proteins inhibit Beclin 1-dependent autophagy. *Cell* 122: 927-939.
71. Tsujimoto Y, Croce CM (1986) Analysis of the structure, transcripts, and protein products of bcl-2, the gene involved in human follicular lymphoma. *Proc Natl Acad Sci USA* 83: 5214-5218.
72. Breitschopf K, Haendeler J, Malchow P, Zeiher A, Dimmeler S (2000) Posttranslational modification of Bcl-2 facilitates its proteasome-dependent degradation: molecular characterization of the involved signaling pathway. *Mol Cell Biol* 20: 1886-1896.
73. Azad N, Vallyathan V, Wang L, Tantishaiyakul V, Stehlik C (2006) S-nitrosylation of Bcl-2 inhibits its ubiquitin-proteasomal degradation. A novel antiapoptotic mechanism that suppresses apoptosis. *J Biol Chem* 281: 34124-34134.

74. Mogga SJ, Mustafa T, Sviland L, Nilsen R (2002) Increased Bcl-2 and reduced Bax expression in infected macrophages in slowly progressive primary murine *Mycobacterium tuberculosis* infection. *Scand J Immunol* 56: 383-391.
75. Klingler K, Tchou-Wong KM, Brändli O, Aston C, Kim R, et al. (1997) Effects of mycobacteria on regulation of apoptosis in mononuclear phagocytes. *Infect Immun* 65: 5272-5278.
76. Perkins ND, Gilmore TD (2006) Good cop, bad cop: the different faces of NF-kappaB. *Cell Death Differ* 13: 759-772.
77. Leemans JC, Thepen T, Weijer S, Florquin S, van Rooijen N, et al. (2005) Macrophages play a dual role during pulmonary tuberculosis in mice. *J Infect Dis* 191: 65-74.